MOUNTAIN-PLAINS CONSORTIUM

MPC 14-266 | Yail Jimmy Kim | April 2014

A Novel Methodology for Quantifying the Performance of Constructed Bridges in Cold Regions

MPC
MOUNTAIN-PLAINS CONSORTIUM

A University Transportation Center sponsored by the U.S. Department of Transportation serving the Mountain-Plains Region. Consortium members:

Colorado State University
North Dakota State University
South Dakota State University
University of Colorado Denver
University of Denver
University of Utah
Utah State University
University of Wyoming

A Novel Methodology for Quantifying the Performance of Constructed Bridges in Cold Regions

Yail Jimmy Kim, Ph.D., P.Eng.

Department of Civil Engineering
University of Colorado Denver
Denver, Colorado

April 2014

Acknowledgments

The Principal Investigator gratefully acknowledges all individuals who contributed to the present research report.

Disclaimer

The contents of this report reflect the work of the author, who is responsible for the facts and the accuracy of the information presented. This document is disseminated under the sponsorship of the Mountain-Plains Consortium in the interest of information exchange. The U.S. Government assumes no liability for the contents or use thereof.

EXECUTIVE SUMMARY

This report presents a two-part research program examining the performance of constructed bridges in a cold region, represented by those in the State of North Dakota, and the behavior of concrete members strengthened with carbon fiber reinforced polymer (CFRP) composite sheets in such a service condition. For the first phase, a total of 1,328 decks are sampled from a 15-year inspection period. These data are statistically characterized and probabilistically analyzed. The importance of timely technical action is discussed to enhance the condition rating of the bridge decks. The stochastic response of the existing decks is effectively represented by Gaussian probability distributions, regardless of inspection years. The performance of the decks tends to converge to a certain state with time. The state-transition of the in-situ decks is identified through the global health index proposed. The second part of the research concerns predictive investigations into the axial behavior of concrete exposed to aggressive service environments. Two types of concrete cylinders are studied: unconfined and confined with CFRP sheets. The aggressive environment and service traffic load are represented by freeze-wet-dry cycles with various levels of instantaneous compression load varying from 0% to 60% of the capacities of the unconfined and confined control concrete. Research approaches include three-dimensional deterministic finite element and probabilistic models, associated with a previously conducted experimental program. The effect of the instantaneous live load is significant on the performance of the unconfined and confined concrete, including the variation of compliance and volumetric characteristics. The efficacy of CFRP-confinement increases when the intensity of the live load increases. Reliability performance of the confined concrete is influenced by the environmental and physical conditioning. Refined design recommendations such as strength reduction factors are proposed to address the detrimental contribution of the environmental and physical attributes to the performance of CFRP-confined concrete, based on a Monte Carlo simulation that can cover over 95% of all possible cases in a normal probability distribution of the confined concrete.

TABLE OF CONTENTS

Part I: Performance of Bridge Decks in a Cold Region

Part II: A Predictive Investigation Associated with Design Recommendations for CFRP-confined Concrete in Aggressive Service Environments

LIST OF FIGURES

LIST OF TABLES

PART I: PERFORMANCE OF BRIDGE DECKS IN A COLD REGION

1. INTRODUCTION

The Federal Highway Administration reports that 527,991 bridges in the nation are in operation without any restrictions, while 3,578 bridges have been closed to all traffic due to their deficient conditions (FHWA 2011). Tragic bridge collapse events occasionally take place as in the case of the I-35W bridge in Minnesota and the Lake View Drive bridge in Pennsylvania (Hao 2010, Kasan and Harries 2013). Adequate inspection and subsequent maintenance/rehabilitation are, therefore, important technical activities to warrant the reliable performance of constructed bridge structures. Bridge decks are more vulnerable to deterioration than other members because they are directly exposed to distressful service environments (e.g., traffic load and deicing agents). Societal and economic impact induced by deteriorated bridge decks is a significant problem facing the infrastructure community. The unit cost of a rehabilitation program has continuously been increasing with time; for example, from $\$768/m^2$ in 1995 to $\$858/m^2$ in 1999 (Yunovich and Thompson 2003). Inadequate condition evaluation can mislead engineers or decision makers to the unnecessary execution of limited funds allocated to preserving constructed facilities. Quantifying the performance of in-situ bridges is a rigorous and challenging task (Xia and Brownjohn 2004). Aktan et al. (1996) discussed general methods to appraise the condition of constructed highway bridges. Several performance factors were elaborated and corresponding assessment methodologies were detailed. A summary of destructive and nondestructive test methods was provided. Morcous et al. (2002) developed a case-based reasoning model to predict the deterioration of bridge decks. The model was formulated in a way that forthcoming events were determined from previous cases having the same physical configurations. A case-history library was established to include specific problems and implemented to generate a trend of deterioration. Bolukbasi et al. (2004) estimated the condition rating of bridge components based on inspection data. Bridge samples were obtained from Illinois and regression lines were created to engage individual ratings with year built. Kim and Yoon (2010) examined the condition of existing bridges and identified the critical sources of bridge deterioration in cold regions. A large database of 5,289 bridges was analyzed using an ordinary least-square multiple linear regression method combined with geographic information system. Parameters considered were year built, average daily traffic, and physical and environmental attributes. For cold region application, concrete bridges showed better performance than steel bridges due to their durable characteristics.

Current evaluation approaches emphasize element-level damage such as local corrosion or regional concrete-spalling of a bridge component. Global performance of a bridge network subjected to specific conditions (e.g., cold region environment) is not readily characterized yet. It is worthwhile to note that the inspection result of a single bridge is deterministic based on the decision of an inspector; whereas, the summation of inspection results obtained from various types of bridges within the network may be stochastic. The reason is attributed to the fact that each bridge has distinct configurations, for example, year built. By expanding a problem domain to a significantly large scale, stochastic deterioration procedures and their consequences engaged with existing bridges exposed to particular circumstances can be elucidated. A rational approach linking a sufficiently large database with probabilistic observations is necessary to address such a fundamental challenge in data acquisition and interpretation of a constructed bridge cluster. This

paper deals with a comprehensive investigation into the performance evaluation of bridge decks situated in a typical cold region. A total of 1,328 bridge decks were sampled for a 15-year inspection period in North Dakota and scrutinized using descriptive statistical analysis. Emphasis was given to the probabilistic distribution of deck ratings and their time-dependent progression. A set of quantified reliability was formulated accordingly.

2. RESEARCH SIGNIFICANCE

Although the bridge management program mandated by the Federal Highway Administration is extensive and informative, specific technical aspects (e.g., time-dependent propagation of bridge deterioration) are limitedly studied. Effort is required to effectively utilize an enormous database supplied from such a management program. Additional insights will then be provided to accomplishing the objective-oriented assessment of existing bridges. For example, by examining the deterioration history of a bridge network subjected to a certain service environment, future performance of constituent bridges can be prognosticated. This paper is part of an ongoing study characterizing the performance of constructed bridges in cold regions and has emphasized the time-dependent transition of deck conditions from a global perspective.

3. BRIDGE EVALUATION METHODS

Several methods are used to evaluate the condition of in-situ bridge members. The following is a summary of selected approaches relevant to the current research.

3.1 National Bridge Inventory

The National Bridge Inventory (NBI) program intends to manage constructed bridges in the nation. It includes a number of technical details and information such as year built, structural categories, operating conditions, geometric properties, and evaluation results. Bridges longer than 20 feet are subjected to the NBI evaluation. The database is updated every two years after the comprehensive assessment of constructed bridges. The NBI uses a 0-9 rating scale (Table I.1) to appraise the condition of bridge components such as deck slabs, superstructures, and substructures. The NBI may be linked with a bridge management software program called *Pontis* that assists a bridge preserving policy. A deteriorated bridge is technically classified as *structurally deficient* if its component requires major rehabilitation (rating ≤ 4). Of interest in deck evaluation are cracking, spalling, chloride contamination, and regional failure such as potholing.

3.2 Bridge Health Index

The concept of *bridge health index* is based on a ratio of the current element value to the total element value (Thompson and Shepard 2010). The health index formulated ranges between 0% and 100%. The NBI deck rating of 6.9 may be comparable to a health index of 84%

(Scherschligt 2005). Many state agencies, such as the California Department of Transportation, adopt the use of such a health index to manage their bridge structures. Jiang and Rens (2010a) employed the bridge health index to evaluate the performance of 615 constructed bridges in the City and County of Denver. According to their study, some limitations were revealed. For example, the indices calculated were not in good agreement between cost and structural defect. It was recommended that the cost aspect of the bridge health index be eliminated and some adjustment factors be used for increasing the contribution of deteriorated bridge elements to the performance quantification of existing bridges (Jiang and Rens 2010b).

4. RESEARCH APPROACH

A multi-phase research approach was employed to understand the time-dependent deterioration of constructed bridge decks in cold regions, represented by those situated in the State of North Dakota. Below is a summary of the approach, including data sampling, statistical observations, and probabilistic modeling.

4.1 Description of Database

The bridge inspection data collected by the North Dakota Department of Transportation were analyzed in this research program. The format of the in-situ data was based on that of the National Bridge Inventory (NBI). Table I.1 shows the condition rating of constructed bridges as per the Federal Highway Administration (FHWA) guideline (FHWA. 1995). Although such an evaluation scale does not provide sufficient details as to inspected bridge members (e.g., critical location), it generally represents the condition of constructed bridge components (Elbehairy 2007). Emphasis of the current study was placed on the bridge decks inspected from 1989 to 2004 at a typical interval of five years, as shown in Table I.2. The number of deck slabs varied from 136 to 499, depending upon the year inspected. It is worthwhile to note that the discrepancy of these deck numbers may not cause technical issues from a statistics point of view because the number of samples is large enough to generate meaningful analysis results.

Table I.1 NBI Condition Rating

Condition rating	Description	Technical action
9	Excellent	No action required
8	Very good	No need of repair
7	Good	Minor maintenance
6	Satisfactory	Major maintenance
5	Fair	Minor rehabilitation
4	Poor	Major rehabilitation
3	Serious	Immediate rehabilitation needed
2	Critical	Traffic to be controlled
1	Immediate failure	Bridge to be closed
0	Failed	Out of service

Table I.2 Performance of In-situ Bridge Decks

Inspection	Year-built	# of bridges inspected	Mean-rating	Stdev-rating
1989	1900-1925	5	5.8	0.8
	1926-1950	37	6.3	1.4
	1951-1975	155	7.0	0.9
	1976-2000	18	8.2	0.6
	Total	215		
1994	1900-1925	16	6.4	0.8
	1926-1950	91	6.3	1.2
	1951-1975	321	7.2	0.9
	1976-2000	50	8.0	0.7
	Total	478		
1999	1900-1925	14	6.3	1.1
	1926-1950	89	6.3	1.2
	1951-1975	339	7.2	0.9
	1976-2000	57	8.0	0.7
	Total	499		
2004	1900-1925	4	6.5	1.3
	1926-1950	20	6.3	1.1
	1951-1975	99	7.2	1.1
	1976-2000	13	7.9	0.8
	Total	136		

4.2 Statistical Characterization

The technical data described above were statistically characterized. The in-situ bridge decks were sorted out according to year built at an interval of 25 years. According to previous research (Sobanjo et al. 2010), constructed bridges may not require major rehabilitation for the first 25 years unless critical events take place. Table I.2 lists the number of bridge decks inspected within the predefined year-built period. To readily observe the transition of deck conditions with time, a simplified scale was proposed, as shown in Table I.3: the NBI ratings were re-organized to five categories; for example, Category 5 means no technical action is necessary, while Categories 4 and 3 need maintenance or rehabilitation activities.

Table I.3 Proposed Categories Based on the NBI Rating

Category	Rating in NBI	Description
5	9 and 8	Good
4	7 and 6	Maintenance (required)
3	3 to 5	Rehabilitation (required)
2	1 and 2	Critical
1	0	Failed

4.3 Probability Modeling and Corresponding Reliability

Given the variation of deck rating is stochastic, a single deterministic investigation may not be sufficient to understand the condition of constructed decks in cold regions. The statistically arranged data were thus probabilistically modeled. The first step was concerned with determining the normal probability distribution of the in-situ database, based on a normality check of the sampled data. The probability distribution with rating $f(r)$ is generated using Eq. I.1:

$$f(r) = \frac{1}{\sigma\sqrt{2\pi}} \exp\left[-\frac{1}{2} \frac{(r_i - \mu)^2}{\sigma^2} \right] \tag{I.1}$$

where σ and μ are the standard deviation and mean of the deck condition in a specific inspection category and r_i is the individual condition rating from 0 to 9. Reliability of the constructed decks, R is defined as

$$R = \text{Prob}\ (C > C_c) \tag{I.2}$$

where C is the deck condition rating and C_c is the threshold rating. For this research, a rating of 5 was accepted as a threshold value.

4.4 Global Health Index

An assessment method modified from the concept of the bridge health index (AASHTO 2003) is proposed to globally examine the time-dependent response of in-situ bridge decks in North Dakota:

$$H_g(t) = \frac{\sum S_i q_i(t)}{\sum q_i(t)} \tag{I.3}$$

where $H_g(t)$ is the time-dependent global health index, S_i is the condition factor, and $q_i(t)$ is the condition rating of the bridge in a specific inspection time. Table I.4 lists condition factors used to calculate the global health index of various bridge decks from State 9 (Excellent) to State 0 (Failed), conforming to the FHWA rating shown in Table I.1.

Table I.4 Condition Factors Proposed

# of state conditions	State 9	State 8	State 7	State 6	State 5	State 4	State 3	State 2	State 1	State 0
10	1	0.9	0.8	0.7	0.6	0.5	0.4	0.3	0.2	0.1

5. DISCUSSION ON THE PERFORMANCE OF CONSTRUCTED DECKS

This section deals with an overview of the in-situ bridge decks sampled and their performance with time, including the variation of deck ratings, probabilistic investigations and quantified reliability, and global health indices of the bridge cluster.

5.1 Bridge Decks Sampled

Figure I.1 shows a summary of the histograms constructed based on the four inspection years ranging from 1989 to 2004. Although the number of the bridge decks was not identical in all cases, their distribution was basically similar. It is noticed that significant construction has been done in North Dakota between 1951 and 1975, during which 68.5% of the bridges were constructed, on average, of the sampled data in Figure I.1. The condition of the bridge decks is given in Figure I.2, depending upon the year of inspection. According to the work performed in 1989 [Figure I.2(a)], 75.7% of the constructed decks were rated 7 or above so that no serious technical action was necessary, while 24.3% of the decks required major maintenance and rehabilitation (i.e., rated 6 or below). Such a trend was generally maintained until an inspection year of 2004 was reached [Figure I.2(b) to (d)]. By and large, the decks rated 7 tended to decrease with year, while those rated 8 increased. For example, 45.5% and 27.4% of the decks in 1989 were rated 7 and 8, respectively; whereas, 41.2% and 33.8% were rated 7 and 8 in 2004, respectively. These observations imply that significant effort has been made toward improving the condition of the in-situ bridge decks in a timely manner. The portion of the rating below 6 corroborates this hypothesis: 24.3% and 19.9% of the decks were rated 6 or below in 1989 and 2004, respectively. Figure I.3 exhibits typical bridge decks deteriorated by corrosion accompanying concrete-spalling [Figure I.3(a)] and repaired [Figure I.3(b)].

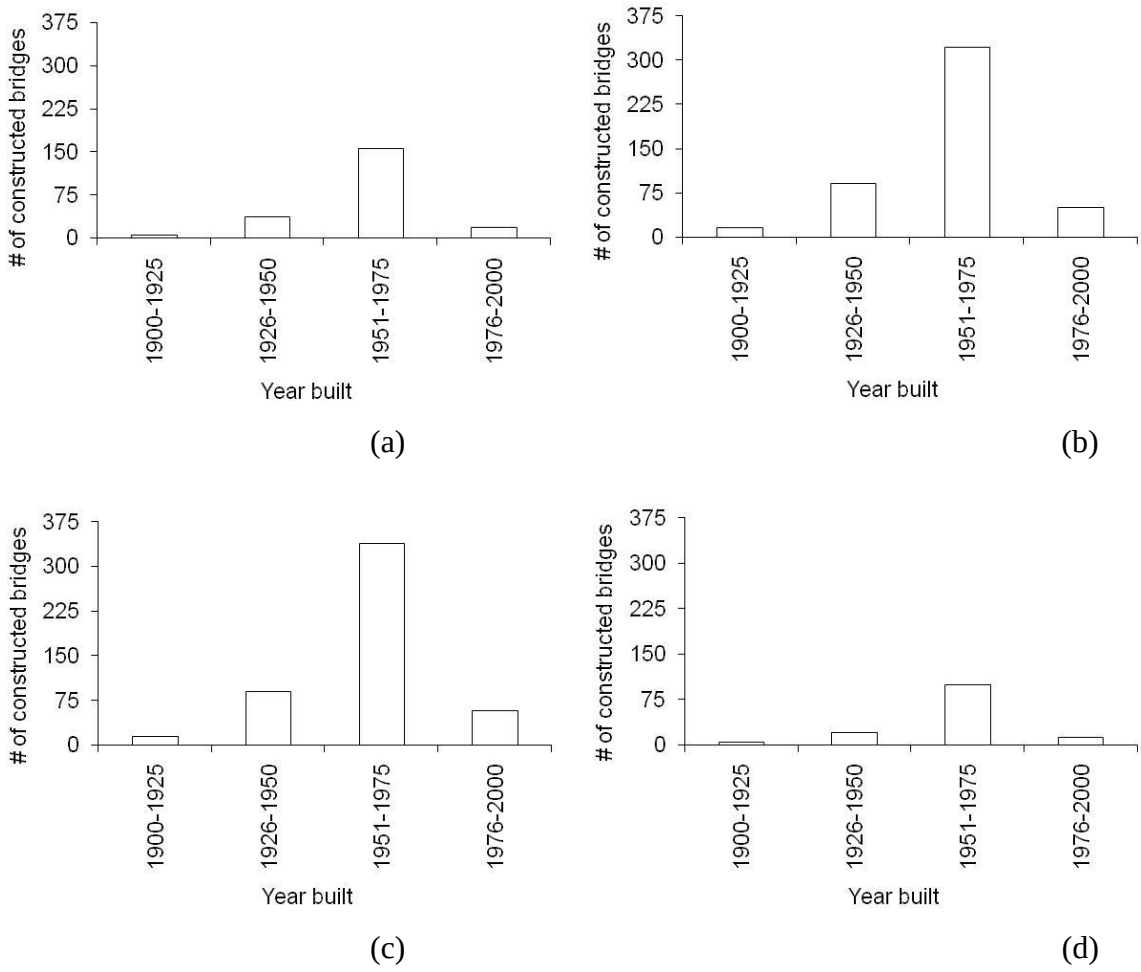

Figure I.1 Number of inspected bridge decks with respect to year built: (a) Database 1989; (b) Database 1994; (c) Database 1999; (d) Database 2004

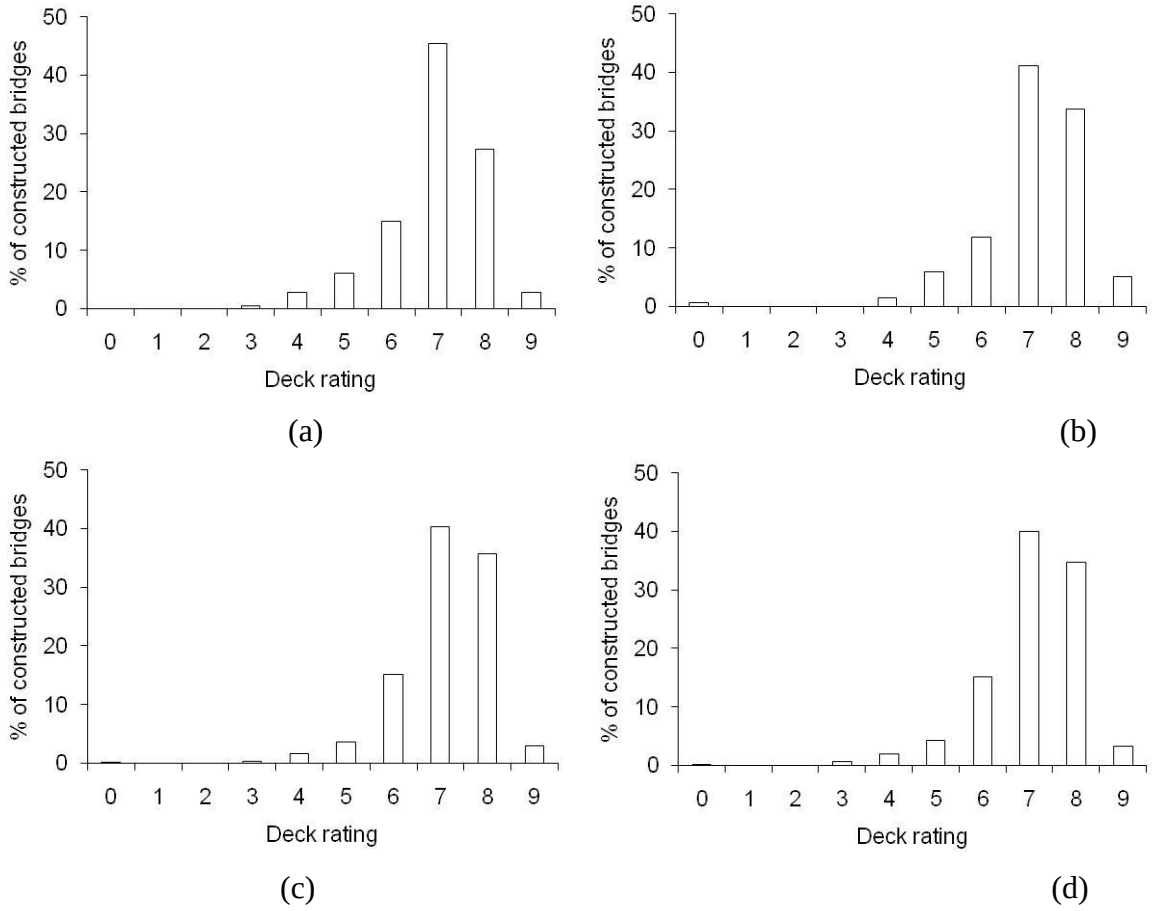

Figure I.2 Distribution of deck rating: (a) Database 1989; (b) Database 1994; (c) Database 1999; (d) Database 2004

(a) (b)

Figure I.3 Deteriorated bridge decks in I-29, North Dakota: (a) corrosion and concrete-spalling; (b) repaired deck

5.2 Performance of Decks with Time

Detailed observations on the distribution of deck ratings are given in Figure I.4. Nonlinear regression lines were added along the upper boundary of the rating data. As discussed earlier, most existing decks were in acceptable conditions (rating ≥ 5). Some decks constructed before 1970 appeared to be critical (rating < 4). These bridges require in-depth assessment and active rehabilitation plans, if necessary. Reconstruction of these bridges seems to be early at this time, given that the design life of a typical bridge is 75 years. The upper boundary regression lines of each inspection year are compared in Figure I.4(e). It is interesting to note that there has been no dramatic change in the regression lines, irrespective of inspection years from 1989 to 2004. Such a result is due to the continued maintenance and rehabilitation activities conducted during this 15-year period, which indirectly shows the effectiveness of timely technical action. Figure I.5 depicts the overall performance evaluation of the decks discussed in Figure I.4. The irregularity in the average rating curves in Figure I.5(a) illustrates the condition rating of the constructed decks was stochastically influenced by a number of parameters, such as the degree of maintenance or rehabilitation, average daily traffic, and use of deicing agents. Nonetheless, an obvious tendency in the variation of average deck ratings with respect to year built was noticed [Figure I.5(a)]: the rating of the decks constructed in the 1900s tended to position in between 5 and 6; whereas, that of the decks built in the 1990s was from 7 to 9. The transition of deck conditions with time is presented in Figure I.5(b). The simplified evaluation scales (Table I.3) were used to readily identify the degree of such transition. For the inspection period of 15 years, the percentage of each rank (i.e., *Good*, *Maintenance*, and so on) was found to be virtually independent of time. For instance, the constructed decks rated the *Maintenance* category were about 55% of the entire decks inspected, while those rated the *Rehabilitation* category were approximately 10%, as shown in Figure I.5(b). It is not clear if these observations were made because the North Dakota Department of Transportation had intentionally controlled the condition rating of the bridge decks when maintenance/rehabilitation decisions were implemented or because all contributing factors to the deterioration of constructed decks (e.g., maintenance frequency, traffic, and weather) had resulted in coincidental results. To understand specific reasons for these transition trends, an extensive parametric analysis may be required using a stochastic modeling approach.

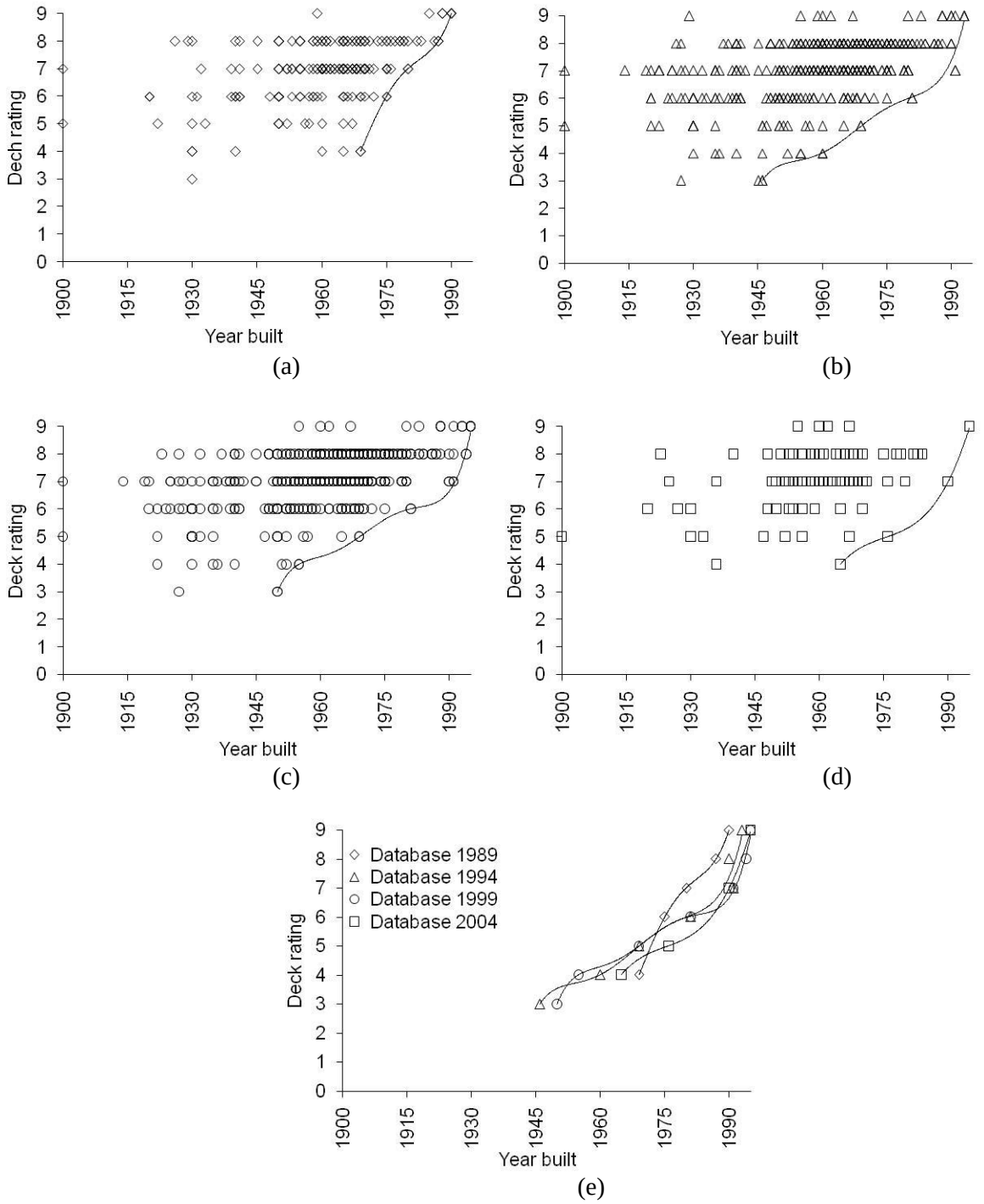

Figure I.4 Distribution of deck ratings with respect to year built: (a) Database 1989; (b) Database 1994; (c) Database 1999; (d) Database 2004; (e) comparison of upper boundary of deck rating

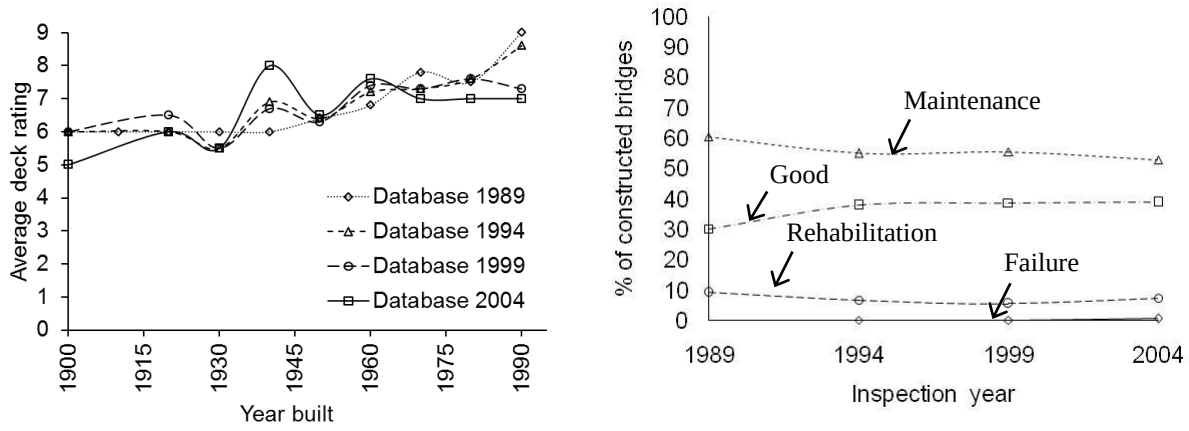

Figure I.5 Variation of deck rating: (a) average rating with respect to year built; (b) condition transition of bridge decks

5.3 Probabilistic Observation in Conjunction with Performance Reliability

The probability distribution of the constructed decks was found to be reasonably *normal*, as shown in Figure I.6, regardless of the inspection year. Figure I.7 exhibits the variation of probability density functions with respect to the year built of the decks at an interval of 25 years. A relatively consistent observation was made in all inspection years. The decks constructed between 1976 and 2000 revealed more concentrated probability density near their mean rating values (i.e., narrow standard deviations) than those built in other time frames. The decks constructed before 1950 demonstrated wide standard deviations in general. Significant uncertainty is expected in these bridge decks, thereby requiring rigorous in-situ evaluation or real-time structural health monitoring. Another interesting finding is that the probability density functions of the decks constructed in the 1900-1925 and 1926-1950 periods tended to merge with time. This indicates that the rating characteristics of existing bridge decks converge to a certain state when their year-built increases, including a mean rating of about 6. The quantified reliability of the constructed decks is given in Figure I.8. The reliability was intended to represent the condition of the entire decks inspected in a specific year so that the global performance of the decks was compared. The performance reliability of the decks was satisfactory: over 90% of the constituent decks demonstrated a rating higher than 5 in all inspection years.

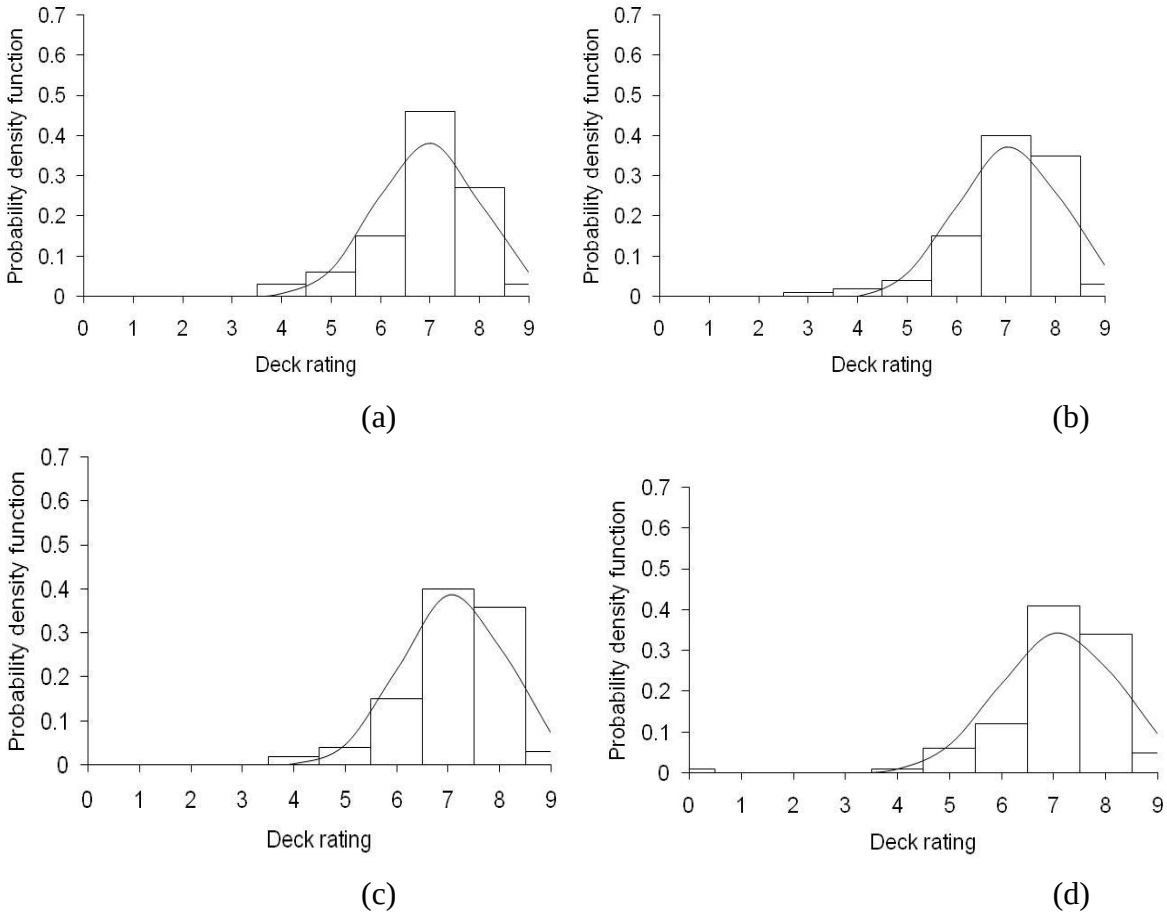

Fig. I.6 Normality check of probability distribution: (a) Database 1989; (b) Database 1994; (c) Database 1999; (d) Database 2004

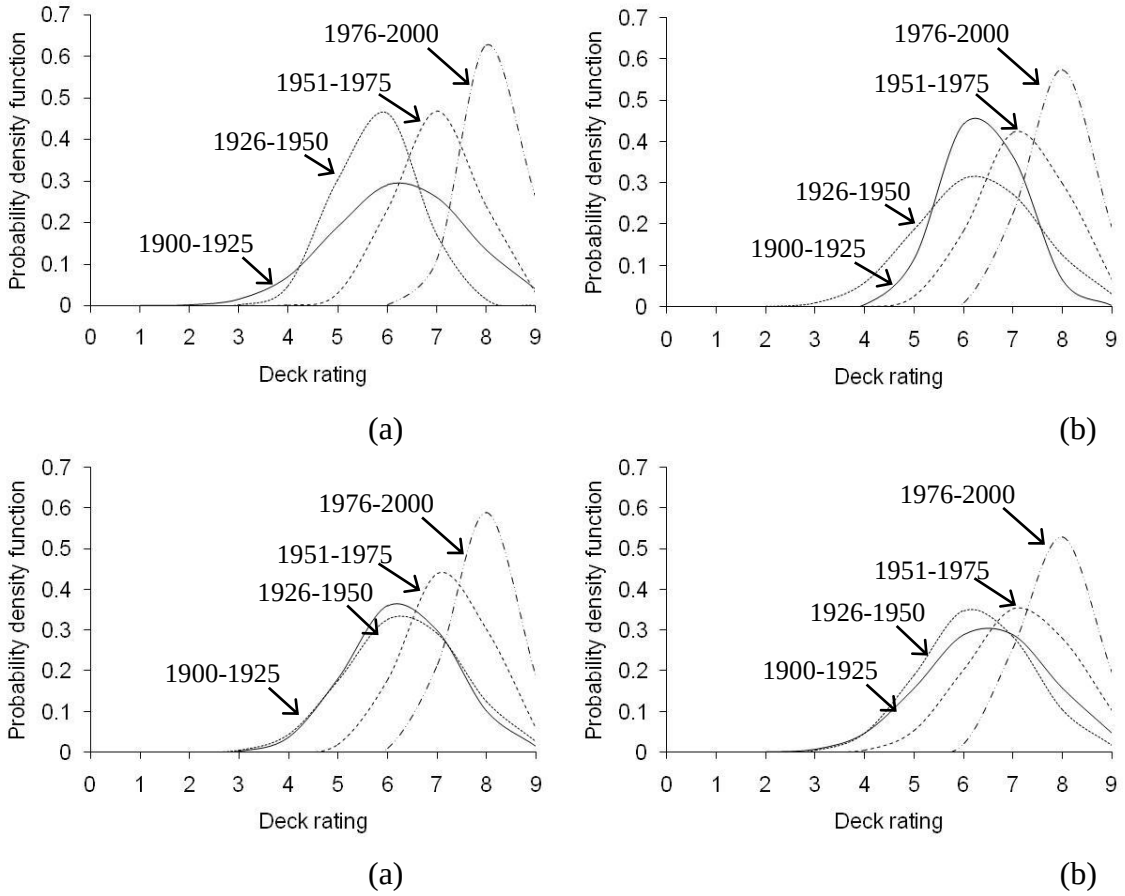

Fig. I.7 Probability density function versus deck rating: (a) Database 1989; (b) Database 1994; (c) Database 1999; (d) Database 2004

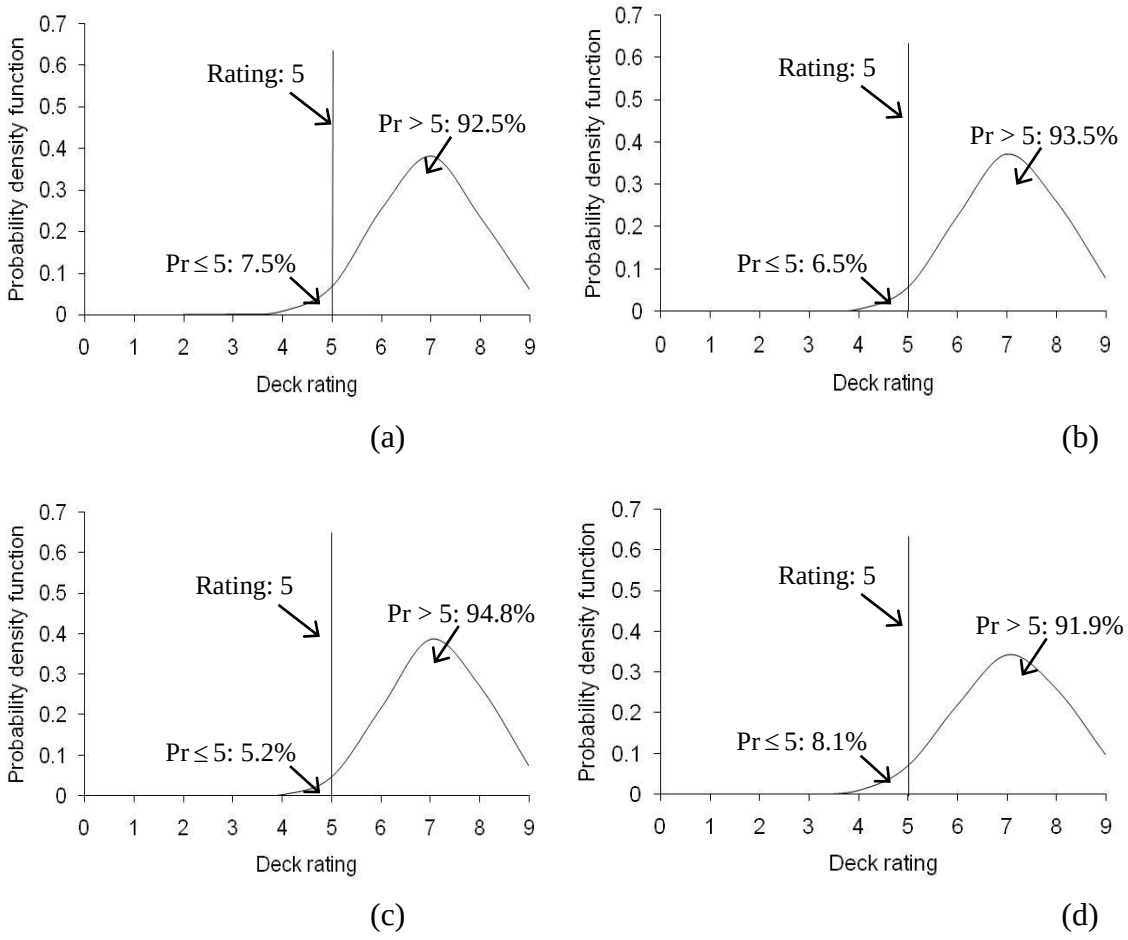

Fig. I.8 Reliability of constructed decks: (a) Database 1989; (b) Database 1994; (c) Database 1999; (d) Database 2004

5.4 Global Health Index

The Global Health Index of the in-situ decks quantified by Eq. I.3 is summarized in Figure I.9. The deck groups constructed in the 1900-1925 and 1926-1950 periods showed average health indices of 72.5% and 73.0%, respectively, while those constructed in the 1951-1975 and 1976-2000 periods exhibited 81.5% and 90.3%, respectively. These observations imply that there was a condition-lag among these construction periods and the lag could be 50 years, which is within the present design life of highway bridges (i.e., 75 years). This estimated condition-lag year may represent the global state-transition of existing bridge decks in cold regions, including the effect of progressive deterioration and corresponding maintenance/rehabilitation activities.

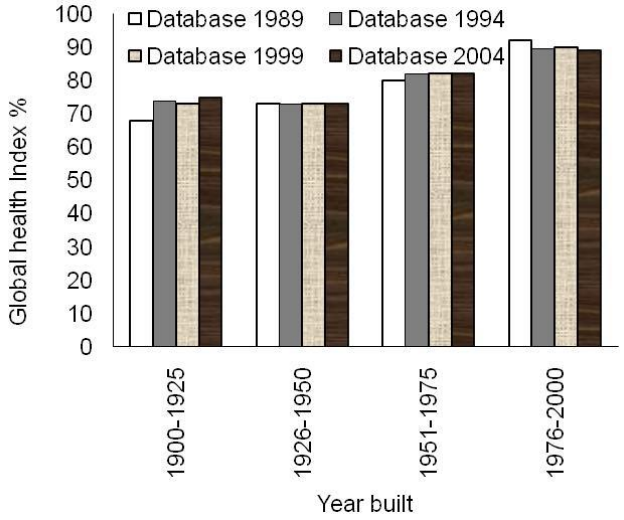

Fig. I.9 Variation of global health index depending upon year-built

Table I.5 Global Health Index for Bridge Decks

Year-built	Global heath index (%)			
	Database 1989	Database 1994	Database 1999	Database 2004
1900-1925	68	74	73	75
1926-1950	73	73	73	73
1951-1975	80	82	82	82
1976-2000	92	90	90	89

Table I.6. Percentage of Constructed Bridges Based on Condition States

Inspection Year	Evaluation category				
	5	4	3	2	1
1989	30.2%	60.5%	9.3%	0.0%	0.0%
1994	38 %	55%	6.8%	0.0%	0.2%
1999	38.7%	55.5%	5.6%	0.0%	0.2%
2004	38.9%	53%	7.4%	0.0%	0.7%

6. SUMMARY AND CONCLUSIONS

This part has presented a methodology evaluating the condition of constructed bridge decks in cold regions through the in-situ data acquired for 15 years in North Dakota. A total of 1,328 decks were sampled and analyzed. The probabilistic approach used provided technical insights into examining existing decks and their reliable performance was quantified accordingly. The following is concluded:

- Timely maintenance of the constructed bridge decks consistently improved their performance rating. The decks constructed before 1970 might need active technical action in conjunction with rigorous evaluation.
- The condition rating of the existing bridge decks was intrinsically stochastic and the concept of probability effectively addressed this complicated issue. Probability distribution of these decks was reasonably Gaussian, irrespective of inspection years. Performance characteristics of the decks in cold regions tended to converge to a certain state with time (i.e., rating of 6) based on the observation of the decks in North Dakota. The proposed global health index identified the state-transition of the constructed decks.

7. REFERENCES

AASHTO. 2003. Pontis bridge management release 4 technical manual, American Association of State Highway and Transportation Officials, Washington, DC.

Aktan, A.E., D.N. Farhey, D.L. Brown, V. Dalal, A.J. Helmicki, V.J. Hunt, and S.J. Shelley. 1996. "Condition assessment for bridge management," *Journal of Infrastructure Systems*, 2(3), 108-117.

Bolukbasi, M., J. Mohammadi, and D. Arditi. 2004. "Estimating the future condition of highway bridge components using National Bridge Inventory data," *Structural Design and Construction*, 9(1), 16-25.

Elbehairy, H. 2007. Bridge management system with integrated life cycle cost optimization, Ph.D. thesis, University of Waterloo, Waterloo, Ontario, Canada.

Hao. S. 2010. "I-35W bridge collapse," *Journal of Bridge Engineering*, 15(5), 608-614.

FHWA. 1995. Recording and coding guide for the structure inventory and appraisal of the nation's bridges, FHWA-PD-96-001, U.S. Department of Transportation, Washington, D.C.

FHWA. 2011. Bridges by posting status, Federal Highway Administration, Washington, DC.

Jiang, X. and K.S. Rens. 2010a. "Bridge health index for city and county of Denver, Colorado. I: current methodology," *Journal of Performance of Constructed Facilities*, 24(6), 580-587.

Jiang, X. and K.L. Rens. 2010b. "Bridge health index for city and county of Denver, Colorado. II: Denver bridge health index," *Journal of Performance of Constructed Facilities*, 24(6), 588-596.

Kasan, J.L. and K.A. Harries. 2013. "Analysis of eccentrically loaded adjacent box girders," *Journal of Bridge Engineering*, 18(1), 15-25.

Kim, Y.J. and D.K. Yoon. 2010. "Identifying Critical Sources of Bridge Deterioration in Cold Regions through the Constructed Bridges in North Dakota," *Journal of Bridge Engineering*, 15(5), 542-552.

Morcous, G., H. Rivard, and A.M. Hanna. 2002. "Modeling bridge deterioration using case-based reasoning," *Journal of Infrastructure Systems*, 8(3), 86-95.

Scherschligt, D.L. 2005. Pontis-based health indices for bridge priority evaluation, 6th National Conference on Transportation Asset Management, Kansas City, MO.

Sobanjo, J., P. Mtenga, and M. Bambo-Roddenberry. 2010. "Reliability-based modeling of bridge deterioration hazards," *Journal of Bridge Engineering*, 15(6), 671-683.

Thompson, P.D. and R.W. Shepard. 2000, AASHTO commonly recognized bridge elements-successful application and lessons learned, Proceedings of the National Workshop on Commonly Recognized Measures for Maintenance, American Association of State Highway Transportation Officials, Washington, D.C.

Xia, P and J. Brownjohn. 2004. "Bridge structural condition assessment using systematically validated finite-element model," *Journal of Bridge Engineering*, 9(5), 418-423.

Yunovich, M. and N.G. Thompson. 2003. "Corrosion of highway bridges: economic impact and control methodologies," *Concrete International*, 25(1), 52-57.

Part II: A Predictive Investigation Associated with Design Recommendations for CFRP-confined Concrete in Aggressive Service Environments

8. INTRODUCTION

Carbon fiber reinforced polymer (CFRP) composites are used to improve the performance of constructed concrete structures. CFRP sheets may be externally bonded to the tensile soffit of a flexural member that needs additional reinforcement and may be wrapped around an axial member to increase load-carrying capacity and ductility. Of interest is the behavior of CFRP-confined (or wrapped) concrete members, such as bridge piers, because the failure of these members may result in the collapse of the entire structure. As such, structural performance of CFRP-confined axial concrete has been extensively studied. Mirmiran et al. (1998) conducted an experimental study to examine the axial behavior of CFRP-confined concrete. Test parameters included concrete strength, fiber volume and orientation, types of adhesives, slenderness ratios, and interfacial characteristics between core concrete and CFRP. A *modified confinement ratio* was used to measure the effectiveness of CFRP-confinement. Geometric properties of confined concrete played a key role in load-carrying capacity; whereas, the effect of bonding agents was negligible. Pessiki et al. (2001) tested various scales of concrete columns confined with CFRP sheets. Stress-strain behavior was examined and the factors affecting axial behavior were identified, namely, the properties of CFRP and the geometry of concrete members. Some empirical approaches were suggested to limit the dilatation of confined concrete. Lam and Teng (2003) developed a design-oriented constitutive relationship for CFRP-confined concrete. A set of test databases was constructed and evaluated using a simple mechanics model, including a number of design parameters such as concrete strength, column dimensions, and CFRP properties. A practical design model was proposed to predict the stress-strain relationship of confined concrete. Fahmy and Wu (2010) evaluated existing predictive models for CFRP-confined concrete. Focus of the study was the changes in stiffness of stress-strain relationships. An experimentally calibrated equation was proposed for the design of CFRP-confined concrete.

Durability performance of CFRP-confined concrete is a crucial factor to consider when CFRP materials are used in aggressive environmental conditions. Karbhari et al. (2000) studied the short-term behavior of CFRP-confined concrete using specimens exposed to 201 cycles of freeze-thaw at temperatures between -20°C and 22.5°C. Mechanical characteristics and failure mode of confined concrete were affected by environmental cycling, including changes in strength and stiffness. Micromechanical response of CFRP was an important issue when subjected to moisture ingress. Teng et al. (2003) monitored in-situ response of FRP-confined bridge piers subjected to aggressive environment. Thermal sensors were installed and visual inspections were regularly performed. Laboratory-scale specimens were also tested to evaluate the behavior of such confined concrete in corrosive and freeze-thaw conditions. FRP-wrapping was found to be effective in protecting the core concrete, and the exposure to freeze-thaw decreased ductility of confined concrete. Toutanji et al. (2007) studied the effect of wet-dry and freeze-thaw on the load-carrying capacity of CFRP-confined concrete specimens. Accelerated conditioning was applied to the specimens; one cycle included six hours of wet-dry and four

hours of freeze-thaw at a temperature of -17.8°C. Test results showed that the strength of CFRP-confined concrete was not significantly influenced by these conditions.

ACI440.2R-08 (ACI 2008a) suggests environmental reduction factors to address the potential degradation of a CFRP system on site. These factors, however, are not object-specific because many factors, such as climate conditions and traffic volume, can contribute to the deterioration of the system Additional research is, therefore, required to suggest refined design provisions. This paper aims to study the durability performance of CFRP-confined concrete when simultaneously subjected to a typical cold region environment and various levels of traffic load, based on predictive modeling. Two-phase investigations, including deterministic and probabilistic approaches, were conducted. Design expressions were developed to enhance the sustainability of CFRP-confined concrete on site.

9. SUMMARY OF EXPERIMENTAL PROGRAM

A concise summary of an experimental program is given in this section, while further details are available in Hossain and Kim (2012). The experimental program evaluated the effect of aggressive environmental conditions associated with live load on the behavior of unconfined and CFRP-confined concrete. The CFRP (equivalent thickness of 0.165 mm) had a nominal tensile strength of 3,800 MPa with tensile modulus of 227 GPa (BASF 2007). Concrete cylinders (75 mm diameter and 150 mm length) were tested in an accelerated durability protocol, consisting of 100 cycles of freeze-wet-dry accompanied by various levels of instantaneous compression load. Figure II.1(a) shows one cycle of the conditioning for 24 hours. The freezing condition for the test cylinders was applied for 16 hours per cycle at a nominal temperature of -30°C [Figure II.1(b)] and the other conditions such as wet and dry were generated at room temperature for eight hours. The level of the instantaneous compression varied from 0% to 60% of the control cylinders' capacity to represent random live load on site. Table II.1 summarizes the details of test categories. Identification code of each case indicates the presence of environmental conditioning and the level of live load (e.g., Env+40% means that the cylinders were environmentally conditioned at an instantaneous load level of 40% of the control capacity). Upon completion of the designed test protocol, all test cylinders were loaded to failure and their residual capacity and strain responses (axial and hoop directions using strain gages) were recorded with a data acquisition system [Figure II.1(c)]. Strength of the unconfined concrete noticeably decreased due to the accelerated conditioning; whereas, the decrease in the confined concrete was insignificant, as shown in Table II.1. CFRP coupons were tested to examine the effect of the environmental conditioning, same as that for the confined cylinders. It was found that the strength of the CFRP was not influenced by the conditioning; however, the tensile modulus (E_{frp}) was reduced as represented by Eq. II.1:

$$E_{frp} = 229.19e^{-0.001N} \text{ in GPa} \quad \text{(II.1)}$$

where N is the number of environmental cycles within the investigation range of the experimental study. The coefficient of variation for the CFRP modulus at 100 cycles was 0.04. The failure mode of the unconfined and confined concrete specimens is given in Figure II.1(d).

Table II.1. Specimen details

Test condition	Specimen ID	Environmental effect	Instantaneous live load effect	Ultimate capacity (MPa)		
				Experiment[1]		Model
				μ	σ	
Unconfined	Control	None	0%	22.9	3.6	22.9
	Env+0%	Yes	0%	20.6	2.3	20.6
	Env+20%	Yes	20%	19.3	3.9	19.3
	Env+40%	Yes	40%	15.1	2.5	15.1
	Env+60%	Yes	60%	13.3	5.0	13.3
Confined	Control	None	0%	79.1	3.3	80.9
	Env+0%	Yes	0%	78.5	5.4	78.9
	Env+20%	Yes	20%	78.8	8.2	77.0
	Env+40%	Yes	40%	76.2	6.0	74.3
	Env+60%	Yes	60%	85.1	2.5	72.6

[1]: μ = mean; σ = standard deviation

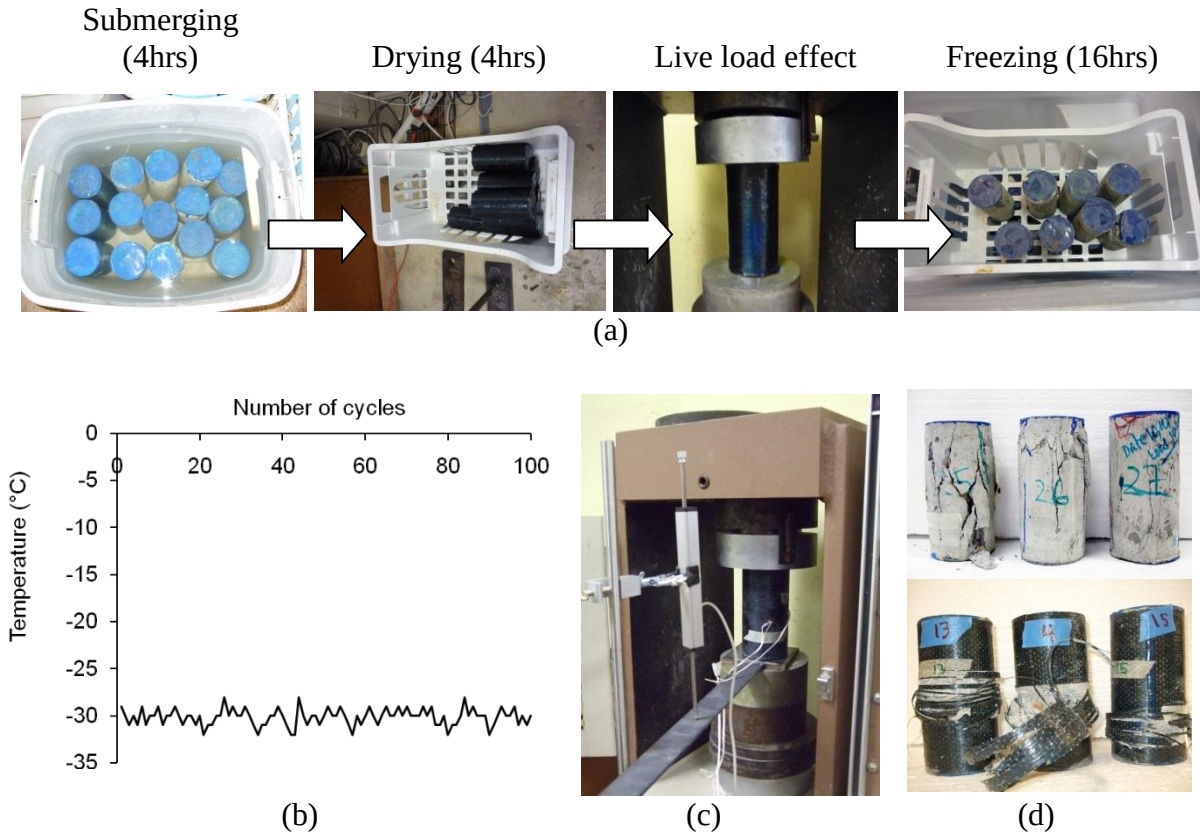

Figure II.1 Test details: (a) one cycle of environmental and physical exposure; (b) measured temperature in environmental chamber; (c) load test and instrumentation; (d) typical failure mode

10. DETERMINISTIC APPROACH

A deterministic investigation was conducted to examine the behavior of unconfined and confined concrete subjected to aggressive service environments [Figure II.1(a)] using a finite element analysis. The following details model development and corresponding findings that are not available in the experimental study described above.

10.1 Model Development

The behavior of the experimental cylinders was predicted using the general purpose finite element program ANSYS, as shown in Figure II.2. Concrete was modeled with eight-node three-dimensional concrete elements (SOLID65), including three translational degrees of freedom per node. The Willam and Warnke model was employed to represent the behavior of the concrete (Willam and Warnke 1975; ANSYS 2011). This model includes the stress state functions ($F / f_c - S \geq 0$ where F is the state function consisting of the principal stresses; f_c is the uniaxial failure strength of the concrete; and S is the failure surface function) and the failure surface function consisting of five components of concrete, as shown in Figure II.2(a). These components comprise ultimate uniaxial tension and compression strengths (f_r and f_c, respectively), ultimate biaxial compression strength (f_{cb} = 1.2 f_c), ambient hydrostatic stress (σ_h), and ultimate compressive strength for states of biaxial and uniaxial compression superimposed on hydrostatic stress state (f_1 = 1.45 f_c and f_2 = 1.725 f_c, respectively). Concrete was assumed to crack when a tensile stress exceeded a predefined limit ($f_r = 7.5\sqrt{f_c}$ in which f_c is the compression strength of the unconfined concrete in psi, ACI 2008b) in any of the orthogonal directions. Once cracking of concrete initiated, isotropic material characteristics of the concrete element changed to orthotropic. The modulus of elasticity was taken as $E_c = 57000\sqrt{f_c}$ in psi (ACI 2008b). The experimentally obtained unconfined concrete strength (f_c) shown in Table II.1 was input to the model so that the constitutive behavior of the concrete subjected to the environmental conditioning and instantaneous live load effects was established on the basis of the Willam and Warnke model (i.e., the five components described above are a function of the compressive concrete strength f_c). It should be noted that the concrete strength of each category was represented by its average strength (e.g., f_c = 19.3 MPa for the unconfined concrete in Env+20%, as shown in Table II.1). The unidirectional CFRP sheet was modeled using three-dimensional spar elements. This two-node element has three translational degrees of freedom per node, which are compatible with those of the concrete element. Displacement compatibility between the concrete and CFRP elements was achieved by a node-sharing technique. The constitutive characteristics of the CFRP were built upon the experimentally measured properties discussed in the *experimental program* section to account for the effect of environmental degradation. A linear stress-strain relationship was assumed for all cases [Figure II.2(a)]. Boundary conditions were given to represent the test condition [translational degrees of freedom were restrained, as shown in Figure II.1(c)] and axial compression load was incrementally applied until failure of the concrete or rupture of the CFRP occurred. A mesh convergence study was carried out to confirm the adequacy of mesh formulation using the unconfined control cylinder, as shown in Figure II.2(c).

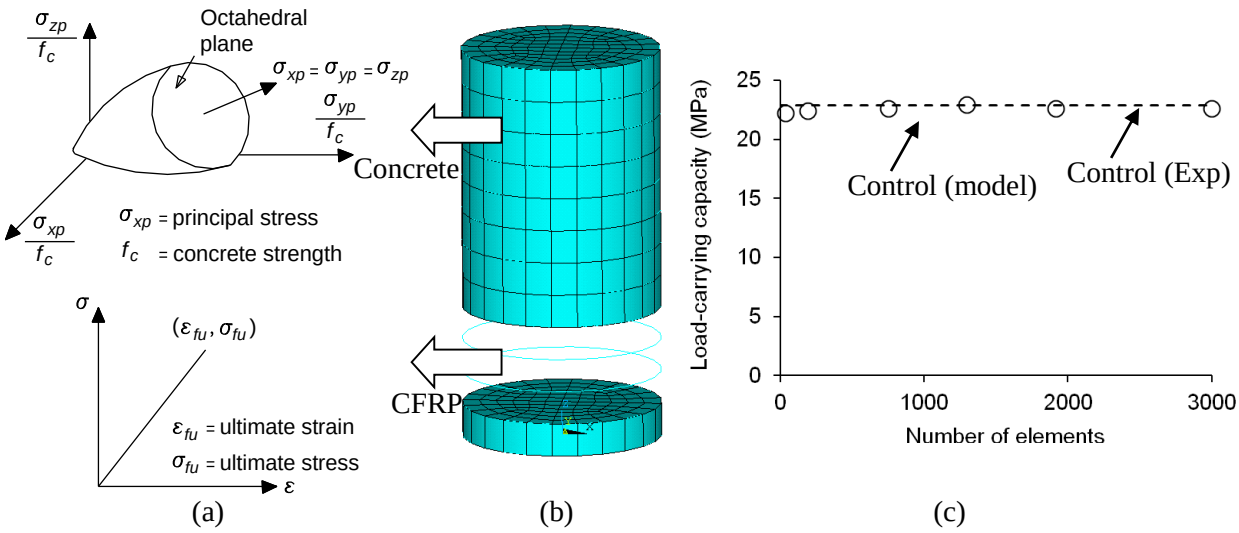

Figure II.2 Numerical modeling: (a) failure criteria; (b) mesh formulation (cutaway view); (c) sensitivity analysis

10.2 Validation of Model

Figure II.3 compares predicted responses of the cylinders with those tested. The axial capacity of the unconfined test cylinders tended to decrease with the increased live load effect and corresponding prediction agreed well with such a trend [Figure II.3(a)]. As for the confined cylinders, the predicted capacity consistently decreased with increasing the load effect and good agreement was made with the experimental counterparts except for Env+60%, which exhibited an increasing capacity [Figure II.3(a)]. This observation may be attributed to the fact that the deteriorated core concrete of these cylinders subjected to Env+60% in the laboratory was engaged when the instantaneous live load effect was applied at every cycle and thus a higher capacity could be noticed. The margin of errors in prediction against test data is shown in Figure II.3(b). The average margin for the cylinders exposed to Env+0% through Env+40% was 8.6%, while the cases in Env+60% showed a relatively large margin of 21.8%, on average. These results demonstrate that the axial behavior of concrete in such a high level of live load is more complicated than the constitutive model used in this study. Effort may be required to develop an improved constitutive relationship for concrete having progressive damage accumulation induced by stochastic live load so that the Willam and Warnke model can be replaced. Stress versus strain responses of the unconfined and confined concrete are given in Figure II.3(c) and (d), respectively (only selected cases are shown here for brevity). The axial strain of the confined concrete was calculated using the axial displacement because the unidirectional CFRP elements were not available to generate axial strains. The predicted strains were reasonably acceptable. Overall, the developed finite element model was adequate to simulate the experimental behavior of CFRP-confined concrete in aggressive environmental conditions.

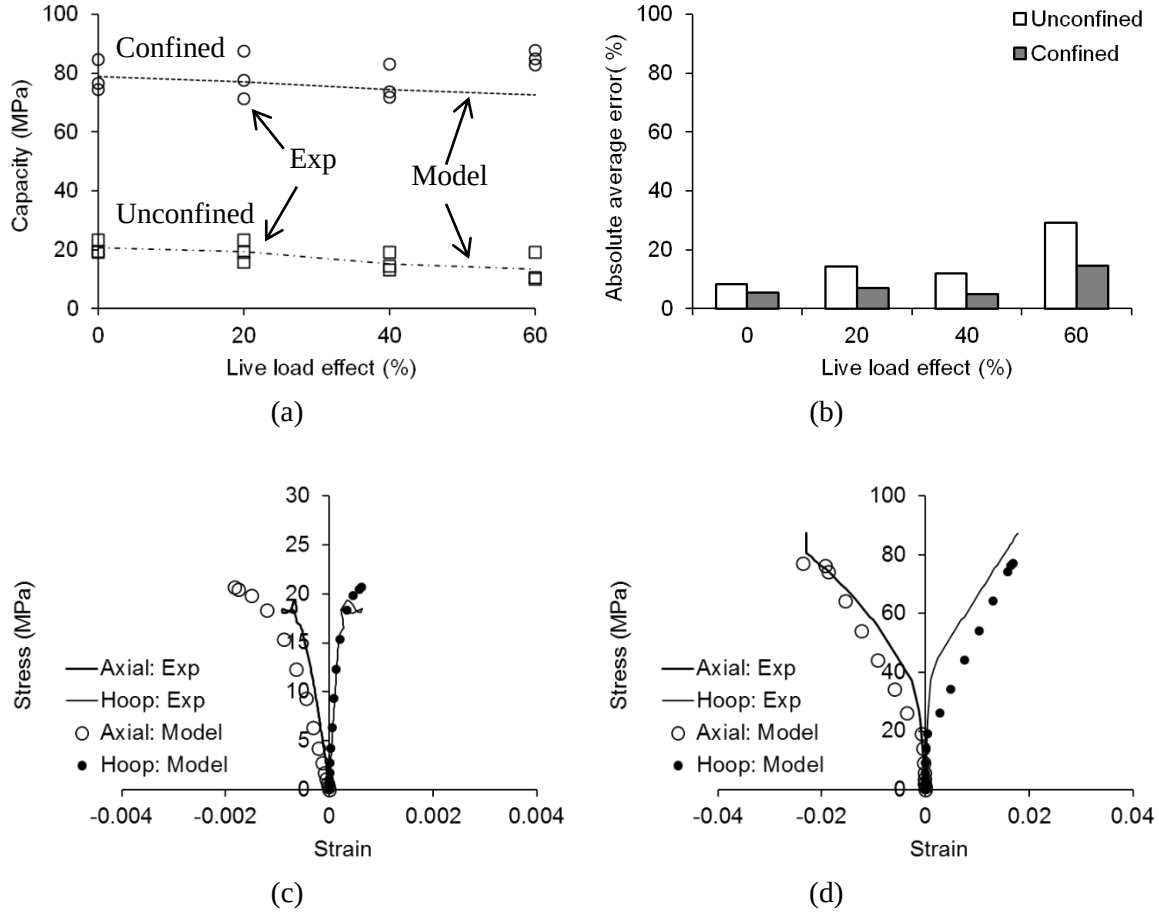

Figure II.3 Validation of predictive model: (a) load-carrying capacity (circle and square = experimental; line = predicted); (b) absolute average error between test and model; (c) stress-strain response of unconfined concrete (Env+0%); (d) stress-strain response of confined concrete (Env+20%)

10.3 Volumetric Change

Figure II.4 shows the predicted variation in volumetric changes of the concrete. The volumetric strain of the cylinders (ε_{vol}) was obtained using Eq. II.2:

$$\varepsilon_{vol} = 2\varepsilon_{\theta} + \varepsilon_{z} \tag{II.2}$$

where ε_{θ} is the hoop strain and ε_{z} is the axial strain. Negative volumetric strains in Figure II.4(a) indicate that the unconfined concrete was in consistent compaction. The rate of volumetric contraction was affected by the level of the instantaneous live load. For the confined concrete, insignificant changes in volumetric strain were observed until the CFRP-confining effect was activated (i.e., before the core concrete reached the unconfined capacity), as shown in Figure II.4(b); however, noticeable increases in the strains were found beyond the thresholds (i.e.,

activation of CFRP confinement). Deterioration of the core concrete subjected to a high level of instantaneous compression influenced the threshold limit. Positive volumetric strains in the confined concrete illustrate that the expansion of the core concrete was effectively controlled so that the ultimate capacity of the concrete significantly increased in comparison with that of the unconfined counterparts (Table II.1). Volumetric strains of the confined cylinders subjected to the live load effect were greater than those of the control at the same load level [Figure II.4(b)]. This observation confirms the core concrete has been damaged during the accelerated environmental conditioning. The changes in dilatation of the confined concrete became unstable when approaching their ultimate stress; in other words, sudden decreases in volumetric strain were observed near the ultimate [Figure II.4(b)]. This illustrates that the volume of the confined cylinders was abruptly reduced. A similar experimental observation was made by others (Samaan et al. 1998).

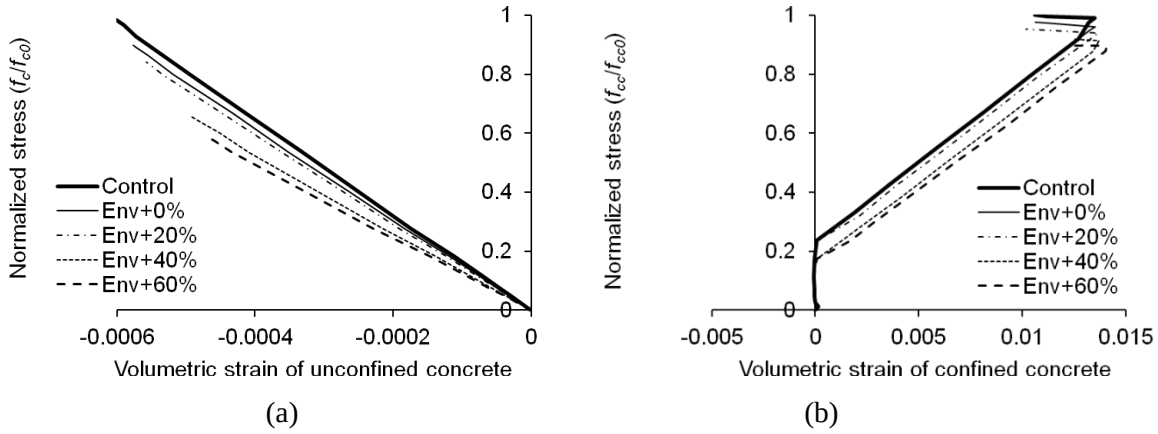

Figure II.4 Variation of volumetric strain: (a) unconfined concrete; (b) confined concrete

10.4 Hoop Strain and Compliance

Figure II.5 shows the development of hoop strains along the confined concrete (only Env+20% is shown here and other cases exhibited similar responses). Almost constant strains were observed along the cylinder at a load level of 25% of the ultimate capacity ($0.25P_u$); whereas, some nonlinearity was noticed with the increased external load. The reduced strains near the ends of the cylinder were well aligned with the failure mode of the confined cylinders where CFRP-rupture occurred outside the end regions [Figure II.1(d)]. Other experimental programs report the same failure trend (Xiao et al. 2010). The variation in predicted compliance of the unconfined and confined cylinders is given in Figure II.6. The compliance of the specimens was obtained using axial strain divided by axial stress. To facilitate a comparison between unconfined and confined cases, the compliance was normalized by the maximum compliance of each case; for example, the normalized compliance of the unconfined concrete subjected to Env+60% was obtained from individual compliance values (due to increasing stresses) divided by the compliance at its ultimate stress. As shown in Figure II.6(a), the normalized compliance of the unconfined concrete was maintained at about 0.55 until the concrete was loaded within an elastic range (e.g., 30% through 50% of f_c/f_{c0} where f_{c0} is the control capacity of the unconfined

concrete); whereas, significant increases in compliance were observed beyond this range. The effect of the instantaneous live load was also a contributing factor. These results imply that the rate of deterioration in unconfined concrete exposed to aggressive service environments is relatively constant when a moderate level of live load (e.g., 30% of the control capacity) is applied; however, a significant increase in the deterioration rate can be accompanied if the concrete is subjected to a higher level of live load. Accumulated damage induced by overload, then, accelerates the failure of the concrete as noticed in Hossain and Kim (2012). For the case of confined concrete [Figure II.6(b)], the constant rate of deterioration was maintained up to about 10% of f_{cc}/f_{cc0} that was equivalent to the elastic range of the unconfined concrete (i.e., 30% to 50% of f_c/f_{c0}). Here, f_{cc0} denotes the control capacity of the confined concrete. Normalized compliance of the confined concrete rapidly increased to 40% of f_{cc}/f_{cc0} and became stable until failure of the concrete was impending. This observation points out that an abrupt increase in deterioration of confined concrete may take place when the CFRP is activated and the rate of deterioration is then softened due to the activated confining effect.

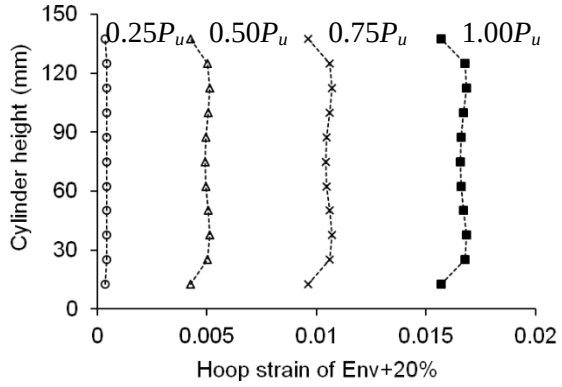

Figure II.5 Hoop strain development of CFRP along confined cylinder

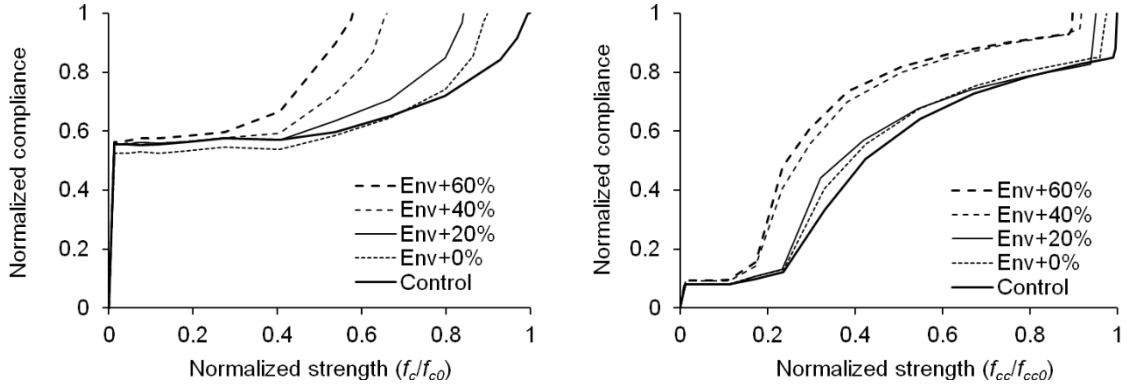

Figure II.6 Variation of compliance: (a) unconfined concrete; (b) confined concrete

11. PROBABILISTIC APPROACH

Live load effects are intrinsically random on the behavior of CFRP-confined axial concrete members on site. To address such uncertainty, a parametric study was conducted using probability theory and the finite element model. The following describes probabilistic approaches and corresponding analysis results.

11.1 Formulation of Probability

To identify the type of probability distribution for the cylinders studied, the median positioning technique with a least-square curve-fitting method was used. The estimated probability that a failure occurs for median plotting positions, $F(f_c, f_{cc})$, may be given in Eq. II.3 (Ebeling 2010).

$$F(f_c, f_{cc}) = \frac{i - 0.3}{n + 0.4} \tag{II.3}$$

where f_c and f_{cc} are the failure capacities of the unconfined and confined cylinders, respectively, and i is the i^{th} specimen of n ordered failure capacities. The z score is obtained using Eq. II.4.

$$z_i = \Phi^{-1}[F(f_c, f_{cc})] \tag{II.4}$$

where $\mathbf{\Phi}$ is the standardized normal probability of the cylinders. If a z score vs. failure capacity (f_c or f_{cc}) plot is linear, it is reasonably assumed that the failure distribution of test specimens is normal [16]. The safety index, β, of the test cylinders is calculated by Eq. II.5.

$$\beta = \frac{R - E}{\sqrt{\sigma_R^2 + \sigma_E^2}} \tag{II.5}$$

where R and E are the mean residual capacity of the test cylinders and the mean instantaneous load applied, respectively, and σ_R and σ_E are the corresponding standard deviations. To compare the safety index of each test category in this research program, the standard deviation of live load (σ_E) was estimated using a coefficient of variation of 0.18 (Nowak 1993). The equation for the normal probability distribution function is shown in Eq. II.6.

$$f(t) = \frac{1}{\sqrt{2\pi\sigma_R}} \exp\left[-\frac{1}{2} \frac{(\{f_c, f_{cc}\} - R)^2}{\sigma_R^2} \right] \tag{II.6}$$

The reliability that a cylinder will function over a failure strength, f_c or f_{cc}, subjected to the environmental and instantaneous load effects is defined as Eq. II.7.

$$R(f_c, f_{cc}) = \Pr\{f_i \geq f_c \text{ or } f_i \geq f_{cc}\} \tag{II.7}$$

where R(f_c,f_{cc}) is the reliability and f_i is the failure capacity of unconfined or confined cylinder *i*. It should be noted that the reliability is a complement of the probability that a cylinder fails.

11.2 Probability Characteristics of Test Cylinders

Figure II.7(a) shows the relationship between the calculated *z* score and the ultimate capacity of the test cylinders based on Hossain and Kim (2012). Both of the unconfined and confined specimens showed a linear trend with coefficients of determination (R^2) of 0.95 and 0.93, respectively. It is, therefore, concluded that the test cylinders used for this research program were normally distributed. Previous research supports such a probability distribution for FRP-strengthened concrete members (Okeil et al. 2002). A comparison of the cumulative distribution function (CDF) between the test and predicted results is made in Figure II.7(b). The standard deviation of the model cylinders was assumed to be the same as that of the test (Table II.1), given that the deterministic finite element model could not provide standard deviations. It is important to note that the number of test specimens will not affect the probability distribution of the cylinders because the distribution has passed the normality test, as shown in Figure II.7(a). The CDF based on the prediction reasonably agreed with that obtained from the test data for the unconfined and confined cylinders (only Env+20% cases are shown in Figure II.7(b) for brevity).

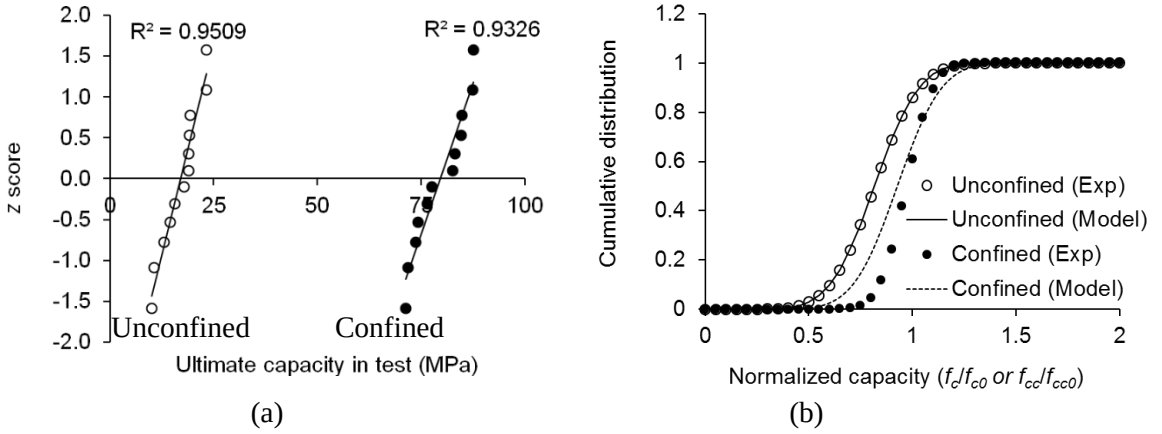

(a) (b)

Figure II.7 Probabilistic response: (a) normality test; (b) comparison of cumulative distribution functions between test and model for Env+20%

11.3 Effect of Instantaneous Live Load

Probability distribution function (PDF) of the predicted cylinders is shown in Figure II.8(a), including the effect of live load on the variation of load-carrying capacity (only Env+0% and Env+60% are presented here). The probabilities that the Env+0% cylinders fail at a lower stress than the control (i.e., f_c/f_{c0} or f_{cc}/f_{cc0} < 1) were 90.2% and 69.5% for the unconfined and confined cases, respectively. When the condition of Env+60% was applied, these probabilities increased

to 97.9% and 72.1%, as shown in Figure II.8(a). These observations indicate that i) the cylinders exposed to instantaneous live load effects tend to fail at a lower external load than those without such effects, ii) the efficacy of CFRP-confinement tends to increase when the load effect increases, and iii) the variability of the cylinders subjected to live load increases due to the increased level of uncertainty. The variation of the safety index β with live load effects is given in Figure II.8(b). Significant drops in β were observed when the instantaneous load effects were present. The unconfined cylinders reached the target safety index $\beta = 2.5$ (AASHTO 2003) in between Env+20% and Env+40%; whereas, the confined ones exhibited substantial improvement. Figures II.8(c) and (d) show the reliability plots of the conditioned cylinders with live load effects. A high reliability (> 0.95) was maintained up to $f_c/f_{c0} = 0.70, 0.50, 0.45, 0.20$ for the unconfined cylinders subjected to Env+0%, +20%, +40%, and +60%, respectively [Figure II.8(c)]. Similar trends were observed for the confined cylinders [Figure II.8(d)]. The level of improved reliability due to CFRP-confinement was more pronounced when the instantaneous load level increased. For example, the reliabilities of the cylinders in Env+60% were 0.13 and 0.63 for the unconfined and confined cases, respectively, to achieve a normalized capacity of 0.8, as shown in Figs. II.8(c) and (d).

11.4 Effect of Constituent Properties

The effect of constituent properties on the reliability of CFRP-confined cylinders was examined to take into account the possible variation of nominal CFRP modulus and concrete strength on site. It was assumed that the standard deviations of these parameters were material properties (Barker and Puckett 1997) and the investigation range varied within ±10% of the nominal values that could happen on site. The modulus of the CFRP did not influence the reliability plot of the confined cylinders, as typically shown in the case of Env+60%, which was the worst case scenario considered in the present study [Figure II.8(e)]. This observation demonstrates that the change in CFRP-modulus can affect the dilatation characteristics of confined concrete; whereas, its contribution to failure is not significant, which agrees with the discussion presented in the *deterministic approach* section. The effect of concrete strength was also insignificant within the range studied here, as shown in Figure II.8(f). This is attributed to the fact that the characteristics of the core concrete changed when the CFRP-confinement was activated and, thus, the strength of the confined cylinders was dominantly governed by the strength of the CFRP, rather than the variation of the concrete strength (i.e., $0.9f_c$ through $1.1f_c$).

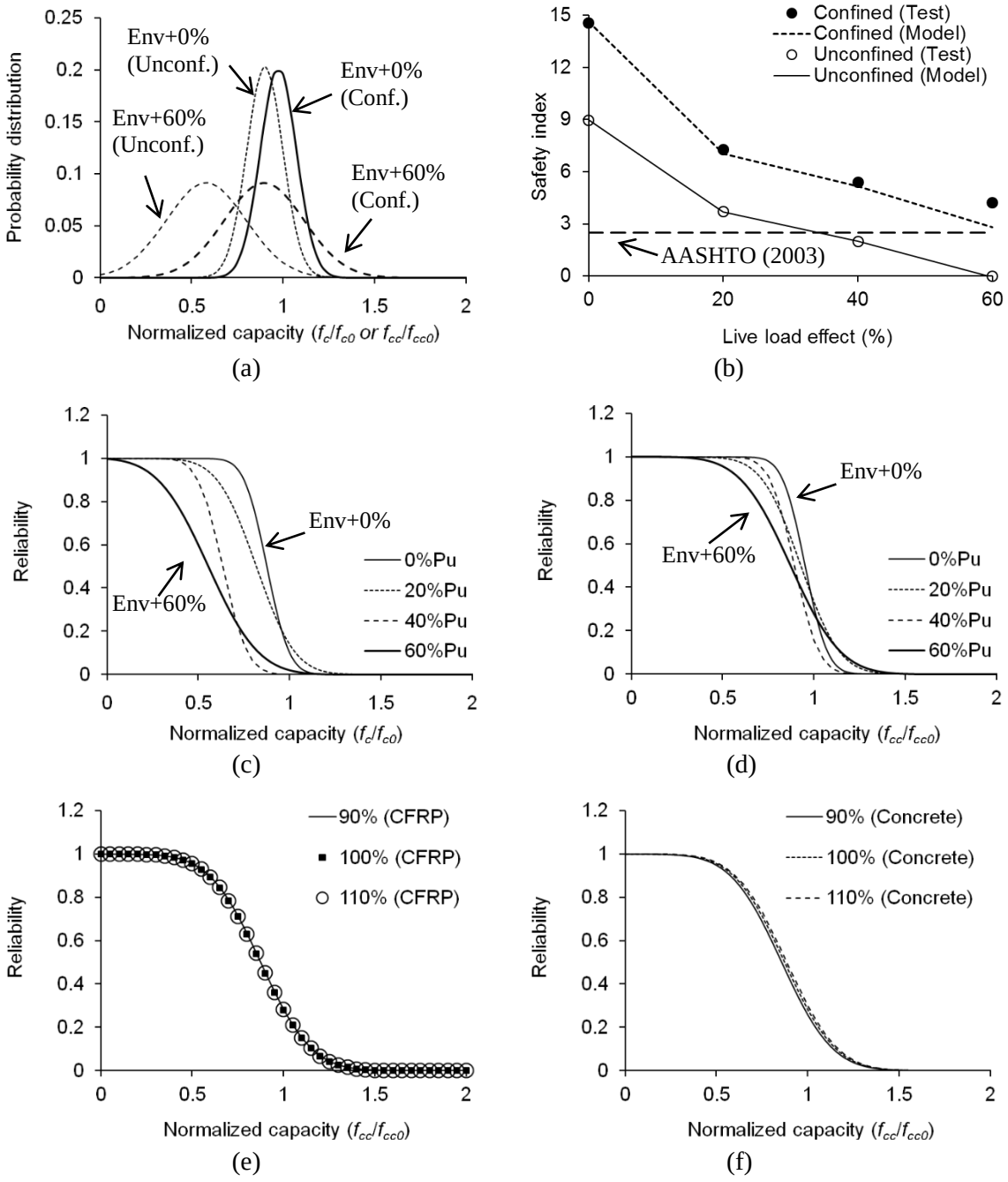

Figure II.8 Parametric study: (a) probability distribution of selected cylinders; (b) safety index; (c) reliability of unconfined cylinders; (d) reliability of confined cylinders; (e) reliability of Env+60% depending on CFRP modulus; (f) reliability of Env+60% depending on concrete strength

12. DESIGN RECOMMENDATIONS

The effect of live load combined with aggressive environments has influenced the behavior of CFRP-confined concrete, as discussed previously. Refined design expressions may, therefore, be required to address this issue for field applications. This section deals with design recommendations for axial concrete members confined with CFRP subjected to cold region conditions.

12.1 Assessment of ACI440.2R-08 Equation

ACI440.2R-08 (ACI 2008a) proposes a design equation to predict the strength of CFRP-confined concrete:

$$f_{cc} = f_c + \psi 3.3\kappa f_l \text{ in which } f_l = C_E \frac{2E_f n t_f \varepsilon_f}{D} \quad \text{(II.8)}$$

where ψ is the FRP reduction factor (= 0.95); κ is the geometric factor (= 1.0 for circular column); C_E is the environmental reduction factor (= 0.85 for CFRP in aggressive environment); E_f and t_f are the elastic modulus and single-ply thickness of the CFRP; n is the number of ply; ε_f is the strain of the CFRP at failure (effective design strain = $0.58\varepsilon_{fu}$ in which ε_{fu} is the ultimate strain of the CFRP); and D is the diameter of the column. To account for the intensity of live load and environmental exposure, the unconfined concrete strength (f_c) and CFRP modulus (E_f) at 100 cycles of the conditioning were taken from Table II.1 and Eq. II.1, respectively. It should be noted that the accelerated durability test presented in the *experimental program* section (i.e., 100 cycles at a 24-hour interval) provides more severe exposure to freeze-thaw than the standard exposure of ASTM C666 (ASTM 2003) and, thus, the degraded material properties obtained from the test program can reasonably be used for design recommendations. The FRP strain at failure (ε_f) was assumed to be its ultimate strain according to previous research (Hossain and Kim 2012). A bias factor was used to assess the margin of Eq. II.8 with respect to the test data:

$$\lambda = \frac{f_{cc-actual}}{f_{cc-predict}} \quad \text{(II.9)}$$

where $f_{cc\text{-}actual}$ and $f_{cc\text{-}predict}$ are the confined concrete strength based on tested and predicted values, respectively. Figure II.9(a) compares the bias factors for ACI440.2R-08 (ACI 2008a). The average bias factors were 1.98 and 1.19 for the cases with and without the contribution of the design factors, respectively. These results indicate that i) the design equation of ACI440.2R-08 can be conservatively applicable (λ = 1.98) to CFRP-confined concrete in cold regions and ii) the nominal expression without design factors may be a reasonable predictor (λ = 1.19) in such circumstances with less computational effort compared with the rigorous finite element model. The statistically obtained bias factor for axial concrete members (λ = 1.14, Siu et al. 1975) agreed well with that of the present research (λ = 1.19). This supports the adequacy of the statistical factors used here even though the number of the test specimens was limited. The average bias factor based on the finite element model was 1.05, as shown in Figure II.9(b).

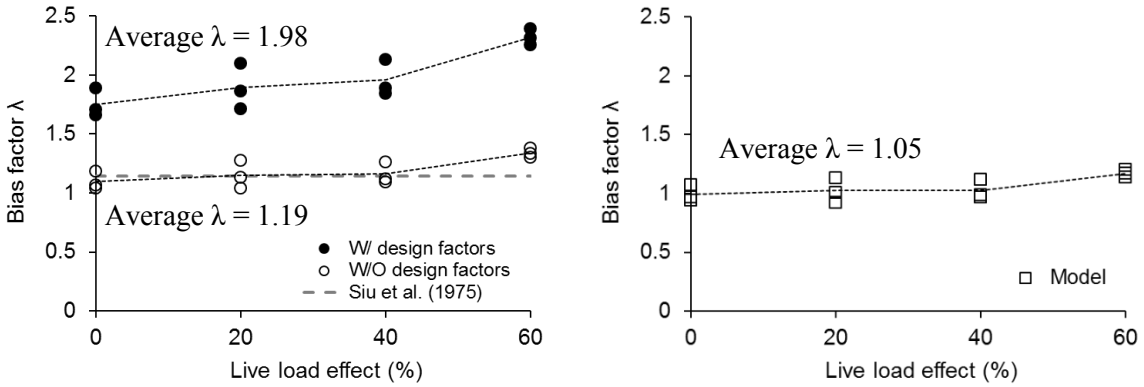

Figure II.9 Assessment of bias factor for strength of confined concrete (circle and square = individual cylinder; line = average): (a) ACI440.2R-08 (ACI 2008a) equation; (b) model

12.2 Monte-Carlo Simulation

A Monte-Carlo simulation was conducted to generate as many data sets as possible to overcome the limitation of the experimental program conducted by Hossain and Kim (2012). This approach is expected to produce realistic design guidelines for CFRP-confined concrete subjected to aggressive environmental conditions associated with various levels of live load. Instead of the computationally expensive three-dimensional finite element models, the ACI440.2R-08 equation without design factors (Eq. II.8) was employed for this research task. To predict the actual capacity of the concrete, the calculated concrete strength confined with CFRP (f_{cc}) was multiplied by the bias factor (λ = 1.19). Material properties such as the strength of the unconfined concrete and the modulus of the CFRP were taken from the test data (Table II.1 and Eq. II.1) within a sampling range of $\mu \pm 3\sigma$ in which μ and σ are the mean and standard deviation of the property, respectively. Figure II.10(a) shows the sampling range of the unconfined concrete strength subjected to Env+0% (for brevity, only this case is shown here, while the mean and standard deviation of all the test categories are available in Table II.1). The modulus of the CFRP was sampled within the same sampling range ($\mu \pm 3\sigma$), as shown in Figure II.10(b), based on the experimentally measured data discussed in the *experimental program* section. The randomly selected properties can cover more than 95% of all possible cases in the entire probability distribution. The variation of geometric properties was not taken into consideration in this research because such effects on the behavior of a CFRP-strengthened system were not significant (Kim and Harries 2012). Figure II.11 exhibits a sensitivity analysis to determine the adequate size of random sampling. The algorithm of the random sampling was generated using the inverse transformation method (Devroye 1986). The number of random samples varied from 5 to 10,000 per test category, as typically shown in the case of Env+0% [Figure II.11(a)]. A convergence of the simulation was made when the sample number was greater than 1,000. The coefficient of variation also tended to converge beyond this limit, as shown in Figure II.11(b). The simulation results of all categories with 10,000 samples were, therefore, taken for the calibration of resistance factors shown in the next section.

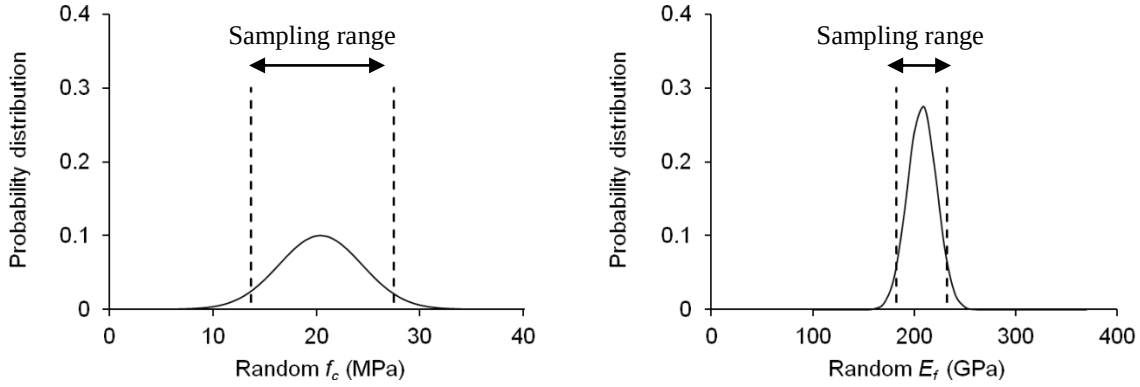

(a) (b)

Figure II.10 Normal distribution of random sampling for Monte-Carlo simulation (Env+0%): (a) unconfined concrete strength; (b) CFRP modulus

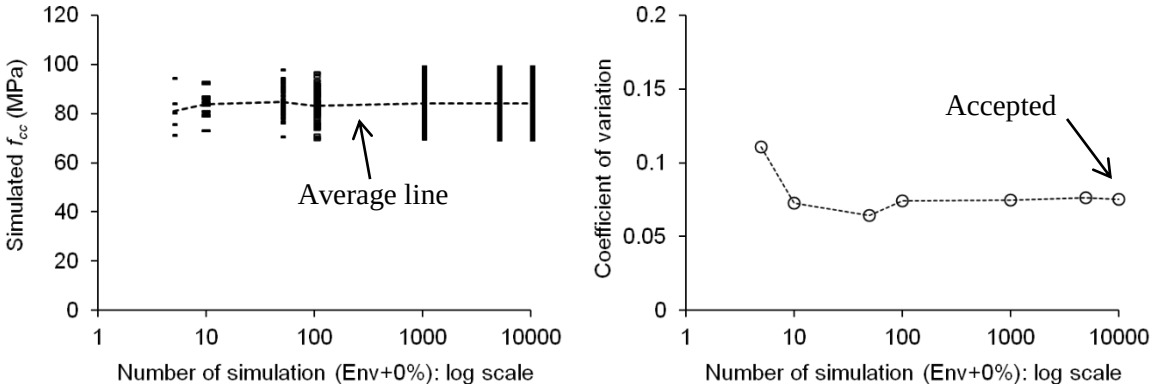

(a) (b)

Figure II.11 Sensitivity analysis of Monte-Carlo simulation: (a) convergence of simulated f_{cc}; (b) coefficient of variance

12.3 Calibration of Resistance Factor

To determine refined resistance factors for CFRP-confined concrete in aggressive service conditions, the following calibration framework was employed. A safety index (β) has been defined as Eq. II.5. The target safety index was set to 2.5 for constructed bridges (AASHTO 2003), which was less than β = 3.5 for the design of a new bridge (AASHTO 2007). The denominator of Eq. II.5 may be approximated as Eq. II.10 (Lind 1971):

$$\sqrt{\sigma_R^2 + \sigma_E^2} = \alpha(\sigma_R + \sigma_E) \tag{II.10}$$

where α is an empirical constant to be determined. Combining Eqs. II.5, II.9, and II.10, the following Load and Resistance Factor Design (LRFD) relationship is obtained (Barker and Puckett 1997):

$$\phi R_n = \gamma E_n \tag{II.11}$$

$$\phi = \lambda_R \left(1 - \alpha\beta V_R\right) \tag{II.12}$$

$$\gamma = \lambda_E \left(1 + \alpha\beta V_E\right) \tag{II.13}$$

where R_n and E_n are the nominal resistance and applied load, respectively, λ_R and λ_E are their bias factors, V_R and V_E are corresponding coefficients of variation, and ϕ and γ are the resistance factor and load factor, respectively. According to the provision of AASHTO (1989), load cases may be classified into four categories that are dependent upon the amount of average daily truck traffic (ADTT). Table II.2 summarizes these categories and corresponding live load factors (γ). The bias factor (λ_E) and the coefficient of variation (V_E) for live load on highway bridges were obtained from previous research (Nowak 1993): 1.15 and 0.18, respectively. The empirical constants (α) were determined using Eq. II.13. The coefficients of variation for each load category (V_R) were obtained from the Monte-Carlo simulation, as shown in Figure II.12. These simulation-based coefficients of variations for the confined concrete were close to those obtained from the experiment except for Env+60%. This is attributed to the fact that the coefficient of variation for the unconfined concrete subjected to Env+60% is greater than that of other cases (Table II.1), and which has influenced the base of the confined concrete (Eq. II.8). The statistically obtained coefficient of variation for axial concrete members (Siu et al. 1975) reasonably agreed with the test data of the unconfined concrete (Figure II.12). The coefficient of variation of CFRP-confined concrete was less than that of unconfined concrete, as shown in Figure II.12. The refined resistance factor (ϕ) for CFRP-confined concrete was calculated using Eq. 12, based on the data obtained from the Monte-Carlo simulation. Figure II.13(a) demonstrates the variation of the resistance factors dependent upon the level of live load. For Category 1 (ADTT less than 1,000 with reasonable control of overload), there was no difference in all load intensities. The effect of live load, however, became obvious when the category number increased so that noticeably low resistance factors were obtained for Category 4 (ADTT greater than 1,000 with ineffective load control). Figure II.13(b) shows the effect of the safety index on the variation of the resistance factors. Note that the resistance factors were averaged here to concisely present the live load effect. There were insignificant differences for the cases with light traffic volume (Category 1); whereas, noticeable drops in the resistance factor were observed when the traffic effect increased. For instance, the average difference between β = 2.5 and 3.5 for Category 1 was 5.8%; however, the difference for Category 4 was 49.1% [Figure 13(b)]. The average resistance factors (ϕ) for a design purpose are summarized in Table II.2, which is aligned with β = 2.5.

Table II.2. Proposed design factors for CFRP-confined concrete in aggressive environments

Category	Condition		Live load factor (γ)[2]	Resistance factor (ϕ)
	ADTT[1]	Overload control		
1	< 1,000	Reasonable	1.30	1.00
2	> 1,000	Reasonable	1.45	0.90
3	< 1,000	ineffective	1.65	0.70
4	> 1,000	ineffective	1.80	0.55

[1] ADTT = average daily truck traffic

[2] factor taken from AASHTO (1989)

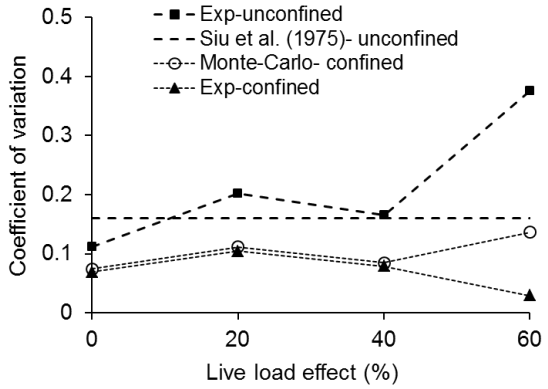

Figure II.12 Generation of COV for CFRP-confined concrete in aggressive environments

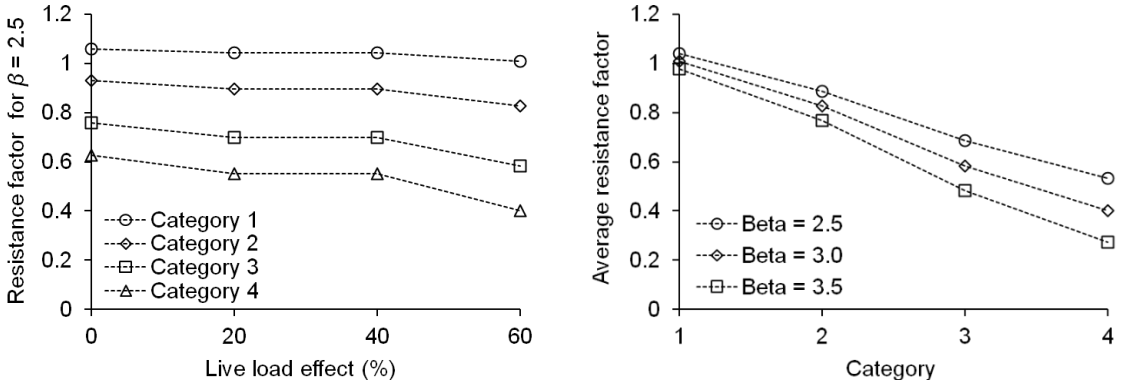

(a) (b)

Figure II.13 Variation of resistance factor for CFRP-confined concrete: (a) individual response with β = 2.5; (b) effect of safety index β

13. SUMMARY AND CONCLUSIONS

Predictive investigations have been carried out to study the behavior of unconfined and CFRP-confined concrete in aggressive service environments. To represent in-situ conditions, an accelerated durability test was conducted with various levels of instantaneous compression load. A three-dimensional finite element model was developed to deterministically examine the response of the specimens, while a simple probability theory was employed to address the random load effects that could take place on site. Refined design parameters were developed based on a Monte-Carlo simulation. The following is concluded:

- The instantaneous live load was a contributing factor to the load-carrying capacity of the concrete. Some end effect was predicted when hoop strains were developed along the confined concrete, which agreed with the experimental failure mode. CFRP-confinement effectively controlled the volumetric changes of the core concrete. The intensity of the live load affected the variation of compliance and the transition of volumetric strains for the unconfined and confined concrete.

- The CFRP-confined concrete tested in the laboratory showed a normal probability distribution. The cumulative distribution function between the test and prediction agreed well. According to the reliability prediction, the level of the instantaneous live load influenced the performance of the unconfined and confined concrete. The efficacy of CFRP-confinement tended to increase with the increased live load intensity. The probability of failure of the conditioned concrete was reduced by the confinement. Reliability performance of the CFRP-confined concrete was more influenced by the external contributions (i.e., environment and live loads) than the variation of the constituent properties within a range of $\pm$ 10% of the nominal values.

- The ACI440.2R-08 [8] equation without design factors was a reasonable predictor for the capacity of the CFRP-confined concrete studied here. The Monte-Carlo simulation covered more than 95% of all possible cases of the confined concrete and generated statistical data to develop design recommendations. The coefficient of variation of the confined concrete was less than that of the unconfined concrete, implying that the CFRP had improved the performance of the core concrete. Refined resistance factors conforming to the provision of AASHTO were proposed for CFRP-confined concrete subjected to aggressive service environments.

14. REFERENCES

AASHTO. 1989. Guide specifications for strength evaluation of existing steel and concrete bridges, American Association of State Highway and Transportation Officials, Washington, D.C.

AASHTO. 2003. Manual for condition evaluation and load and resistance factor rating of highway bridges, American Association of State Highway and Transportation Officials, Washington, D.C.

AASHTO. 2007. AASHTO LRFD bridge design specifications 4th Ed., American Association of State Highway and Transportation Officials, Washington, D.C.

ACI. 2008a. Guide for the design and construction of externally bonded FRP systems for strengthening concrete structures (ACI-440.2R-08), American Concrete Institute, Farmington Hills, MI.

ACI. 2008b. Building code requirements for structural concrete and commentary (ACI-318), American Concrete Institute, Farmington Hills, MI.

ANSYS. 2011. On-line manual, ANSYS Inc., Canonsburg, PA.

ASTM. 2003. Standard test method for resistance of concrete to rapid freezing and thawing (ASTMC 666M), American Society for Testing and Materials, West Conshohocken, PA.

Barker, R.M. and J.A. Puckett. 1997. Design of highway bridges based on AASHTO LRFD bridge design specifications. John Wiley & Sons, Inc., New York, NY.

BASF. 2007. MBrace® CF130 Unidirectional high strength carbon fiber fabric for the MBrace composite strengthening system, BASF Construction Chemicals, Shakopee, MN.

Devroye, L. 1986. Non-uniform random variate generation, Springer-Verlag, New York, NY.

Ebeling, C.E. 2010. An introduction to reliability and maintainability engineering (2nd Ed.), Waveland Press, Inc. Long Grove, IL.

Fahmy, M.F.M. and Z. Wu. 2010. Evaluating and proposing models of circular concrete columns confined with different FRP composites, Composites Part B, 41, 199-213.

Hossain, M. and Y.J. Kim. 2012. "Instantaneous load intensities incorporated with a cold region environment for CFRP-confined concrete in axial compression," *Journal of Composites for Construction*, 16(4), 440-450.

Karbhari, V.M., J. Rivera, and P.K. Dutta. 2000. "Effect of short-term freeze-thaw cycling on composite confined concrete," *Journal of Composites for Construction*, 4(4), 191-197.

Kim, Y.J. and K.A. Harries. 2012. “Predictive response of notched steel beams repaired with CFRP strips including bond-slip behavior,” *International Journal of Structural Stability and Dynamics*, 12(1), 1-21.

Lam, L. and J.G. Teng. 2003. “Design-oriented stress-strain model for FRP-confined concrete,” *Construction and Building Materials*, 17, 471-489.

Lind, N.C. 1971. “Consistent partial safety factors,” *Journal of the Structural Division*, ASCE, 97, 1651-1669.

Mirmiran, A., M. Shahawy, M. Samaan, H. El Echary, J.C. Mastrapa, and O. Pico. 1998. “Effect of column parameters on FRP-confined concrete,” *Journal of Composites for Construction*, 2(4), 175-185.

Nowak, A.J. 1993. Calibration of LRFD bridge design code, NCHRP-12-33, Transportation Research Board, Washington, D.C.

Pessiki, S., K.A. Harries, J.T. Kestner, R. Sause, and J.M. Ricles. 2001. “Axial behavior of reinforced concrete columns confined with FRP jackets,” *Journal of Composites for Construction*, 5(4), 237-245.

Okeil, A.M., S. El-Tawil, and M. Shahawy. 2002. “Flexural reliability of reinforced concrete bridge girders strengthened with carbon fiber-reinforced polymer laminates,” *Journal of Bridge Engineering*, 7(5), 290-299.

Samaan, M., A. Mirmiran, and M. Shahawy. 1998. “Model of concrete confined by fiber composites,” *Journal of Structural Engineering*, 124(9), 1025-1031.

Teng, M.-H., E.D. Sotelino, and W.-F. Chen. 2003. “Performance evaluation of reinforced concrete bridge columns wrapped with fiber reinforced polymers,” *Journal of Composites for Construction*, 7(2), 83-92.

Siu, W.W.C., S.R. Parimi, and N.C. Lind. 1975. “Practical approach to code calibration,” *Journal of the Structural Division*, ASCE, 101, 1469-1480.

Toutanji, H.A., L. Zhao, and G.J. Isaacs. 2007. “Durability studies on concrete columns confined with advanced fibre composites,” *International Journal of Materials and Product Technology*, 28(1/2), 8-28.

Willam, K.J. and E.D. Warnke. 1975. Constitutive model for the triaxial behavior of concrete, Proceedings of the International Association for Bridge and Structural Engineering, 19, Bergamo, Italy, 1-30.

Xiao, Q.G., J.G. Teng, and T. Yu. 2010. “Behavior and modeling of confined high-strength concrete,” *Journal of Composites for Construction*, 14(3), 249-259.

LIST OF ACRONYMS AND ABBREVIATIONS

C	=	deck condition rating
C_c	=	threshold rating
C_E	=	environmental reduction factor
D	=	diameter of column
E	=	mean instantaneous load applied
E_c	=	modulus of elasticity of concrete
E_f	=	elastic modulus of CFRP
E_n	=	applied load
F	=	state function consisting of the principal stresses
f_r	=	ultimate uniaxial tension strength of concrete
f_c	=	ultimate uniaxial compression strength of concrete
f_{cc}	=	failure capacity of confined cylinders
f_{cc0}	=	control capacity of the confined concrete
$f_{cc\text{-}actual}$	=	confined concrete strength based on tested value
$f_{cc\text{-}predict}$	=	confined concrete strength based on predicted value
f_i	=	failure capacity of unconfined or confined cylinder i
f_1	=	ultimate compressive strength for states of biaxial compression superimposed on hydrostatic stress state
f_2	=	ultimate compressive strength for states of uniaxial compression superimposed on hydrostatic stress state
$H_g(t)$	=	time-dependent global health index
N	=	number of environmental cycles within the investigation range of the experimental study
n	=	number of ply
P_u	=	ultimate capacity
$q_i(t)$	=	condition rating of the bridge in a specific inspection time
R	=	reliability of the constructed decks or mean residual capacity of test cylinder
$R(f_c,f_{cc})$	=	reliability
R^2	=	coefficients of determination
R_n	=	nominal resistance
r_i	=	individual condition rating from 0 to 9
S	=	failure surface function
S_i	=	condition factor
t_f	=	single-ply thickness of CFRP
V_E	=	coefficients of variation for applied load
V_R	=	coefficients of variation for nominal resistance
α	=	empirical constant
β	=	safety index

γ = load factor
ε_θ = hoop strains
ε_z = axial strain
ε_f = strain of CFRP at failure
ε_{fu} = ultimate strain of CFRP
κ = geometric factor
λ = bias factor
λ_E = bias factor for applied load
λ_R = bias factor for nominal resistance
μ = mean of the deck condition in a specific inspection category
σ = standard deviation of the deck condition in a specific inspection category
σ_E = standard deviation of mean instantaneous load applied
σ_h = ambient hydrostatic stress
σ_R = standard deviation of mean residual capacity of test cylinder
$\mathbf{\Phi}$ = standardized normal probability of cylinders
ϕ = resistance factor
ψ = FRP reduction factor